THE JOURNAL OF COMPARATIVE NEUROLOGY 331:14-36 (1993)

Distribution of Parvalbumin-Immunoreactive Cells and Fibers in the Monkey Temporal Lobe: The Amygdaloid Complex

ASLA PITKÄNEN AND DAVID G. AMARAL
University of Kuopio, Department of Neurology, Kuopio, Finland (A.P.); and
The Salk Institute, Laboratory of Neuronal Structure and Function, La Jolla, California 92037 (A.P., D.G.A.)

ABSTRACT

The calcium-binding protein parvalbumin was immunohistochemically localized in the monkey amygdaloid complex. Parvalbumin-immunoreactive neuronal cell bodies, fibers, and terminals were observed in several amygdaloid nuclei and cortical areas. Three types of aspiny neurons, ranging from small spherical cells (Type 1) to large multipolar cells (Type 2) and fusiform cells (Type 3) were observed in most amygdaloid regions, though the proportions of the cell types were different in each region. The density of parvalbumin-immunoreactive fibers and terminals tended to parallel the density of labeled cell bodies. The highest densities of parvalbumin profiles were observed in the nucleus of the lateral olfactory tract, the periamygdaloid cortex (PAC2), the magnocellular division of the basal nucleus, the ventrolateral portion of the lateral nucleus, and the accessory basal nucleus. The regions containing the lowest densities of parvalbumin-positive profiles were the medial nucleus, anterior cortical nucleus, central nucleus, and the paralaminar nucleus. In regions with fiber and terminal labeling, pericellular networks of fibers, reminiscent of basket cell terminations, were commonly observed to surround unstained neuronal cell bodies and proximal dendrites. In the magnocellular division of the basal nucleus, and to a lesser extent in the lateral nucleus, parvalbumin-labeled "cartridges" of axo-axonic terminals were observed on the initial segments of unlabeled cells. Parvalbumin-positive varicosities were also commonly observed in close apposition to the soma and dendrites of parvalbumin-immunoreactive cells. Given the close correspondence between the distribution of parvalbumin-positive neurons and a subset of GABAergic neurons in many brain regions, these data provide a first indication of the organization of the inhibitory circuitry of the primate amygdaloid complex.

Key words: amygdala, calcium-binding protein, immunohistochemistry, interneurons, primate

The primate amygdaloid complex is a heterogeneous structure composed of at least 13 nuclei and cortical areas (Amaral et al., '92). Cytoarchitectonic, chemoarchitectonic, and connectional studies indicate that these different amygdaloid regions each have unique anatomical characteristics. In particular, each region appears to generate a unique complement of intrinsic and extrinsic connections. Despite recent increased interest in the neurobiology of the amygdaloid complex, remarkable gaps remain in basic data concerning amygdaloid circuitry. Little is known, for example, concerning the organization of the inhibitory intrinsic circuitry of the amygdala and whether inhibitory connections are entirely intranuclear or extend from one amygdaloid region to another. As part of an ongoing analysis of the intrinsic connections of the monkey amygdala, we have carried out a series of studies aimed at identifying the morphology and distribution of inhibitory neurons in the amygdala. The present study describes neurons and fiber systems identified with antibodies to the calcium-binding protein, parvalbumin.

Parvalbumin-like immunoreactivity occurs in a subpopulation of neurons in a variety of brain regions (Celio, '90) including the cerebral cortex (Celio, '86; DeFelipe et al., '89; Hendry et al., '89; Van Brederode et al., '90; Demeulemeester et al., '91a), the septal nuclei (Freund, '89), the

Accepted December 14, 1992.

Address reprint requests to Dr. David G. Amaral, Laboratory of Neuronal Structure and Function, The Salk Institute, P.O. Box 85800, San Diego, CA 92186-5800.

hippocampal formation (Kosaka et al., '87; Katsumaru et al., '88), and the striatum (Cowan et al., '90; Waldvogel et al., '91). In each of these regions, parvalbumin-immunoreactive neurons are also positive for markers associated with GABAergic neurotransmission. Interestingly, the parvalbumin-positive GABAergic neurons are generally different from the GABAergic neurons that colocalize peptide neuromodulators such as somatostatin (Nitsch et al., '90), neuropeptide Y (Nitsch and Leranth, '91) or cholecystokinin (Katsumaru et al., '88; Gulyas et al., '91). Consistent with the notion that parvalbumin-immunoreactive cells are GABAergic is the finding that they are typically aspiny nonpyramidal cells. In most areas, however, they form a heterogeneous population. In the monkey cerebral cortex, for example, parvalbumin immunoreactivity is found both in basket and chandelier cells (Hendry et al., '89; Lewis and Lund, '90; Van Brederode et al., '90).

Because of their capacity for buffering the intracellular concentration of calcium, it has been proposed that calcium-binding proteins confer resistance to certain forms of traumatic cell death associated with excitotoxic injury and epileptic episodes (Sloviter, '89; Kamphuis et al., '89; Weiss et al., '90). Sloviter et al. ('91) have recently demonstrated, for example, that parvalbumin-positive intrinsic neurons in the human hippocampal formation are preferentially preserved in cases of temporal lobe epilepsy. The case for this type of protection during ischemia has remained rather controversial, however. Clearly, there are populations of neurons in the hippocampal formation, for example, that have high levels of the calcium-binding proteins, yet are vulnerable to transient periods of ischemia (Mudrick and Baimbridge, '89; Freund et al., '90; Johansen et al., '90). While several studies have elucidated the distribution of parvalbumin-immunoreactive cells and fibers in the rat brain (Celio, '90 and references therein), substantially fewer studies have been carried out in the primate (Hendry et al., '89; Blümcke et al., '90; Lewis and Lund, '90; Van Brederode et al., '90; Huntley and Jones, '90; Hendrickson et al., '91; Nitsch and Leranth, '91; Sloviter et al., '91; Seress et al., '91). In particular, no comprehensive survey of the distribution of calcium-binding proteins has been published for the primate temporal lobe. This is of substantial interest since temporal lobe structures are implicated in a variety of clinically relevant pathologies such as epilepsy and Alzheimer's disease. In this series of studies, we first describe the distribution of parvalbumin-immunoreactive cell bodies, fibers, and terminal plexuses in the different nuclei of the monkey amygdaloid complex. This will be followed by a parallel analysis of the primate hippocampal formation. In subsequent papers we will report on the distribution of other calcium-binding proteins as well as on the localization of markers for GABAergic cells and processes.

MATERIALS AND METHODS

Animals and fixation

The brains of three *Macaca fascicularis* monkeys (M7-90, M8-90, M11-90, weight 2.9–5.2 kg) were prepared for the demonstration of parvalbumin-like immunoreactivity. The monkeys were perfused intracardially by using a pH-shift fixation protocol (Berod et al., '81). Animals were deeply anesthetized with ketamine HCl (10 mg/kg, i.m.) followed by sodium pentobarbital (50 mg/kg, i.p.). The animals were sacrificed by transcardial perfusion of the following solutions: 0.9% saline (250 ml/min for 2 minutes); 4% paraformaldehyde in 0.1 M sodium acetate buffer, pH 6.5 (250 ml/min for 5 minutes and 100 ml/min for 15 minutes) and 4% paraformaldehyde in 0.1 M sodium borate buffer, pH 9.5 (100 ml/min for 30 minutes). The brains were blocked stereotaxically and postfixed in the final fixative for 6 hours. The brains were then cryoprotected in 10% glycerol with 2% dimethylsulfoxide (DMSO) in 0.1 M sodium phosphate buffer for 1 day followed by 20% glycerol with 2% DMSO in 0.1% sodium phosphate buffer for 3 days. The brains were frozen with cooled isopentane (Rosene et al., '86) and stored at −70°C until further processing. Each brain was cut in the coronal plane at 30 μm section thickness on a freezing sliding microtome. Sections were stored in tissue collecting solution (TCS: 30% ethylene glycol, 25% glycerin in 0.05 M sodium phosphate buffer) at −20°C or −70°C prior to immunohistochemical staining.

Immunohistochemical procedures

Sections from two of the brains (M8-90, M11-90) were stained by the peroxidase-antiperoxidase (PAP) method and sections from the third brain (M7-90) were stained by the avidin-biotin technique.

Peroxidase-antiperoxidase method. Whole free-floating coronal sections were collected from the TCS and washed three times in 0.02 M potassium phosphate buffer, pH 7.4 (KPBS). To block nonspecific binding, the sections were incubated in a solution containing 10% normal rabbit serum and 0.5% Triton X-100 in 0.02 M KPBS for 4 hours at room temperature. Thereafter, the sections were incubated in a solution that contained monoclonal mouse

Abbreviations

AAA	anterior amygdaloid area
AB	accessory basal nucleus
ABmc	accessory basal nucleus, magnocellular division
ABpc	accessory basal nucleus, parvicellular division
ABvm	ventromedial division
AHA	amygdalohippocampal area
Bi	basal nucleus, intermediate division
Bmc	basal nucleus, magnocellular division
Bpc	basal nucleus, parvicellular division
CE	central nucleus
CEl	central nucleus, lateral division
CEm	central nucleus, medial division
COa	anterior cortical nucleus
COp	posterior cortical nucleus
DAB	3′,3′-diaminobenzidine
DMSO	dimethylsulfoxide
GABA	γ-aminobutyric acid
I	intercalated nucleus
L	lateral nucleus
Lvl	lateral nucleus, ventrolateral division
Ldm	lateral nucleus, dorsomedial division
M	medial nucleus
NLOT	nucleus of the lateral olfactory tract
PAC2	periamygdaloid cortex 2
PAC3	periamygdaloid cortex 3
PACs	periamygdaloid cortex, sulcal portion
PAP	peroxidase-antiperoxidase
PL	paralaminar nucleus
PU	putamen
TCS	tissue collecting solution

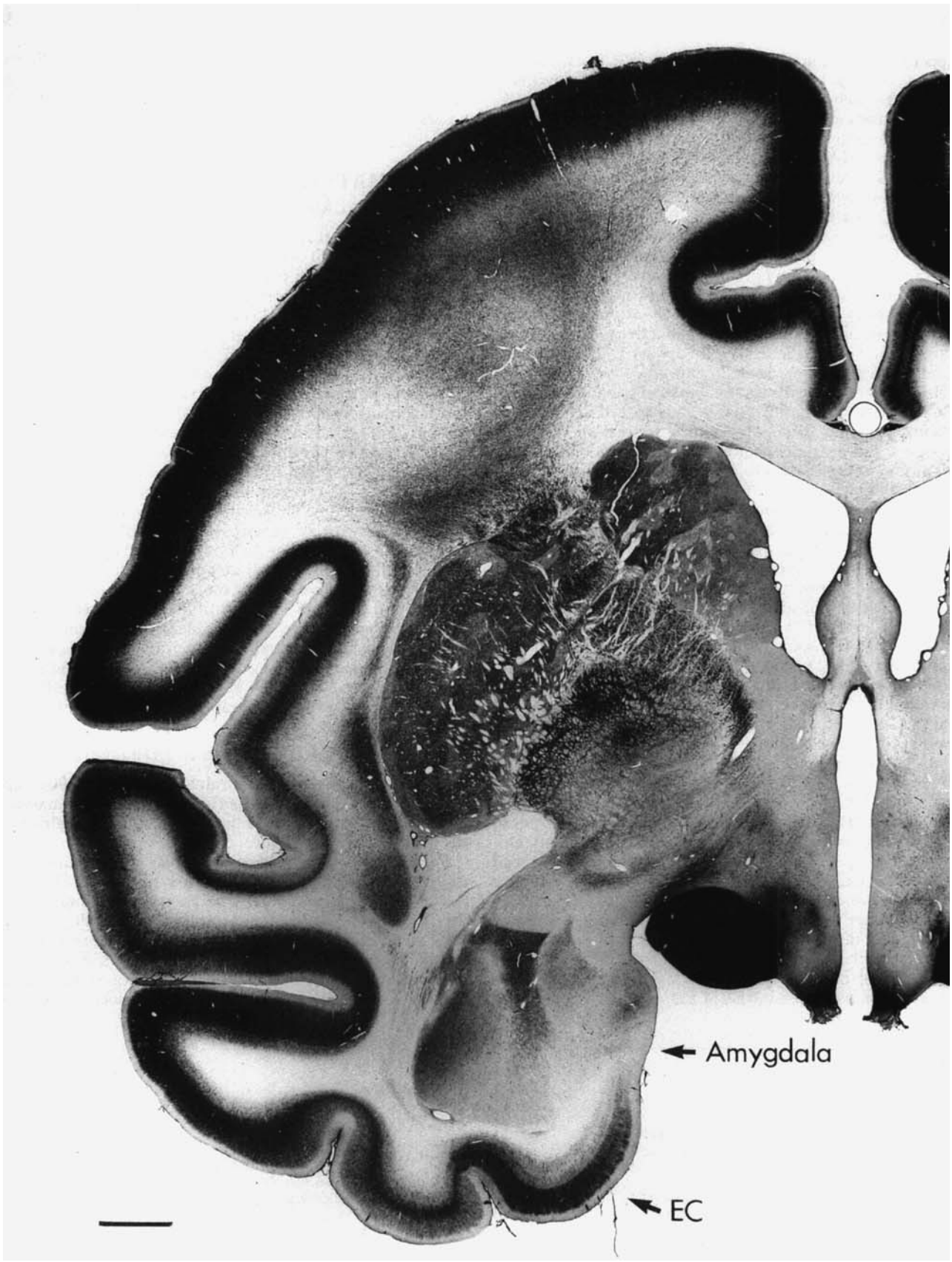

Fig. 1. Low power photomicrograph of a hemisphere of the monkey brain at the level of the amygdala. This coronal section provides an overview of the distribution of parvalbumin immunoreactivity in the amygdaloid complex. Note the relatively low level of staining in the amygdala compared with the adjacent cortical (such as the entorhinal cortex, EC) and subcortical regions. Bar = 2 mm.

anti-carp muscle parvalbumin (No. 235, kindly provided by Dr. Marco Celio, University of Zürich, Switzerland; Celio et al., '88) (diluted 1:1,000–1:10,000), 0.5% Triton X-100 and 1% normal rabbit serum in 0.02 M KPBS for 60 hours at 4°C. Following incubation in the primary antiserum, the sections were washed three times (30 minutes each) in 0.1 M Tris-buffered saline (TBS), pH 7.2 and incubated in a solution containing rabbit anti-mouse IgG (1:30) (ICN 65-157), 1% normal rabbit serum and 0.2% Triton X-100 in 0.1 M TBS, pH 7.2 for 4 hours at room temperature. The sections were again washed and then incubated overnight at 4°C in a solution that contained mouse PAP (1:100) (Sternberger Monoclonals, #45, Jarretsville, MD), 1% normal rabbit serum and 0.2% Triton X-100 in 0.1 SEM TBS, pH 7.2. After further washing, the sections were incubated with DAB (Cappel, #31845, Durham, NC) (0.05% DAB and 0.01% H_2O_2 in 0.1 M TBS, pH 7.6). The sections were rinsed three times for 10 minutes each and mounted on gelatin-coated slides, dried overnight, defatted, hydrated and intensified with OsO_4 and thiocarbohydrazide by the method of Lewis et al. ('86).

Avidin-biotin method. The sections were blocked and incubated in the primary antiserum as described above except that the normal rabbit serum was replaced with normal horse serum. Following the two-day incubation in the primary antiserum, the sections were washed three times for 10 minutes each in 0.02 M KPBS containing 2% normal horse serum. Thereafter, the sections were incubated in a solution containing horse biotinylated anti-mouse IgG (Vector, BA-2000, Burlingame, CA), 1% normal horse serum and 0.3% Triton X-100 in 0.02 M KPBS, pH 7.4 for 1 hour at room temperature. The sections were washed twice as described before and incubated for 45 minutes at room temperature in avidin-biotin solution (diluted 1:25) (BioStain basic kit, Biomeda, CA) in 0.02 M KPBS, pH 7.4. After two washes, the sections were recycled into the secondary antibody solution for 45 minutes and avidin-biotin solution for 30 minutes. The sections were washed three times in 0.02 M KPBS, pH 7.4 and reacted with DAB (0.05% DAB and 0.04% H_2O_2 in 0.02 M KPBS, pH 7.4), washed three times in 0.02 M KPBS and intensified as described earlier.

The characterization of the antibody used in these studies has been described in detail (Celio et al., '88). In the present study, control sections were incubated without the primary antibody, which resulted in the complete absence of stained profiles. To aid in the delimitation of nuclei in the amygdala, an adjacent series of sections was stained with thionin. A subset of the parvalbumin-stained sections were also counterstained with thionin.

Analysis of immunohistochemically prepared tissue

The sections were analyzed with a Leitz Dialux 20 microscope with both brightfield and darkfield optical systems. The distribution of parvalbumin-immunoreactive cell bodies in a representative series of coronal sections from one of the cases (M11-90) was plotted by means of a computer-aided digitizing system (Minnesota Datametrics, St. Paul, MN). Camera lucida drawings from the adjacent Nissl-stained sections were used to define the various nuclei of the amygdala and the outline and plots were superimposed by using the Canvas (Daneba, Miami, FL) software package on a Macintosh computer. To illustrate the morphological subtypes of parvalbumin-immunoreactive cells, camera lucida drawings were made (1,590×) of representative cells found in the lateral nucleus of the amygdala.

It became clear during early stages of the analysis that the parvalbumin-positive cells formed a heterogeneous population of amygdaloid cells. To aid in the description of these cells, we measured the cross-sectional areas of a sample of cells (n = 1,520) from a representative section of the lateral nucleus, basal nucleus, accessory basal nucleus (from the section illustrated in Fig. 4B), nucleus of the lateral olfactory tract (Fig. 2B), PAC2, PAC3, PACs and the amygdalohippocampal area. For these measurements, cells were drawn with the aid of a camera lucida with a 100× objective. The area of each cellular profile was calculated with a digitizing tablet and SigmaScan software on an IBM computer. Statistical analysis was carried out with the Statview program on the Macintosh computer. ANOVA was used to determine differences in cell size between the types of parvalbumin-labeled cells both in the amygdala as a whole and in the different nuclei of the amygdala. Differences in the mean cell size of the three cell classes were evaluated with the Student's two-tailed t-test for unpaired samples.

Low power darkfield and brightfield photomicrographs were taken with a Nikon Multiphot 4 × 5 inch system. Higher magnification photomicrographs were taken with a Leitz Dialux 20 microscope equipped with a Wild MPS camera system. Additional photomicrographs were taken using Nomarski optics.

RESULTS

Nomenclature of amygdaloid nuclei and cortical areas

We have previously provided detailed descriptions of the nomenclature used in this paper for the primate amygdaloid complex (Price et al., '87; Amaral et al., '92). The various amygdaloid areas are indicated in the Nissl-stained sections in Figures 2–7. Briefly, the deep nuclei include the lateral nucleus (which we have subdivided into ventrolateral and dorsomedial divisions), the basal nucleus (subdivided into magnocellular, intermediate and parvicellular divisions), the accessory basal nucleus (partitioned into magnocellular, parvicellular and ventromedial divisions), and the paralaminar nucleus. The superficial nuclei include the anterior cortical nucleus, the medial nucleus, the nucleus of the lateral olfactory tract, the periamygdaloid cortex (which can be subdivided into at least three subregions; PACs, PAC2 and PAC3), and the posterior cortical nucleus. The remaining nuclei consist of the anterior amygdaloid area, the central nucleus (which is divided into lateral and medial subdivisions), the amygdalohippocampal

Figs. 2–7. (On following pages.) Representative coronal sections through the monkey amygdala arranged from rostral (Figs. 2 and 3) to caudal (Figs. 7 and 8). Each of the three levels through the amygdala is represented in 4 panels. Panels **2A, 4A** and **6A** are brightfield photomicrographs of a Nissl-stained section. Panels **2B, 4B** and **6B**, respectively, are brightfield photomicrographs of the adjacent section stained immunohistochemically for the distribution of parvalbumin. Panels **3A, 5A** and **7A** are computer-generated plots of the distribution of parvalbumin-immunoreactive cell bodies observed in the section illustrated in 2B, 4B and 6B, respectively. Panels **3B, 5B** and **7B** are darkfield photomicrographs of the same section illustrated in 2B, 4B and 6B, respectively. The darkfield image highlights the distribution of parvalbumin-immunoreactive fibers and terminals. Bars = 1 mm.

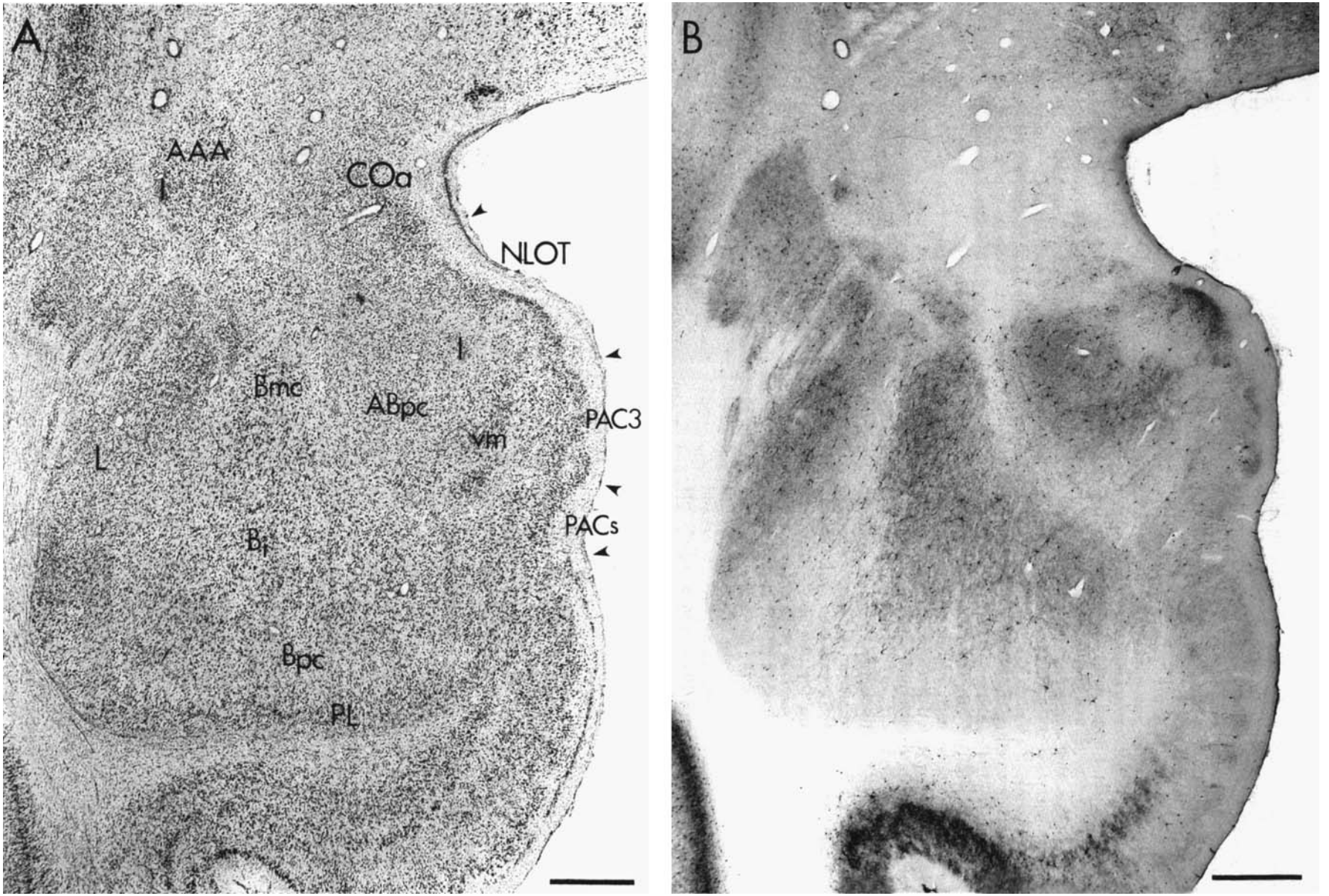

Figure 2 (See legend, p. 17)

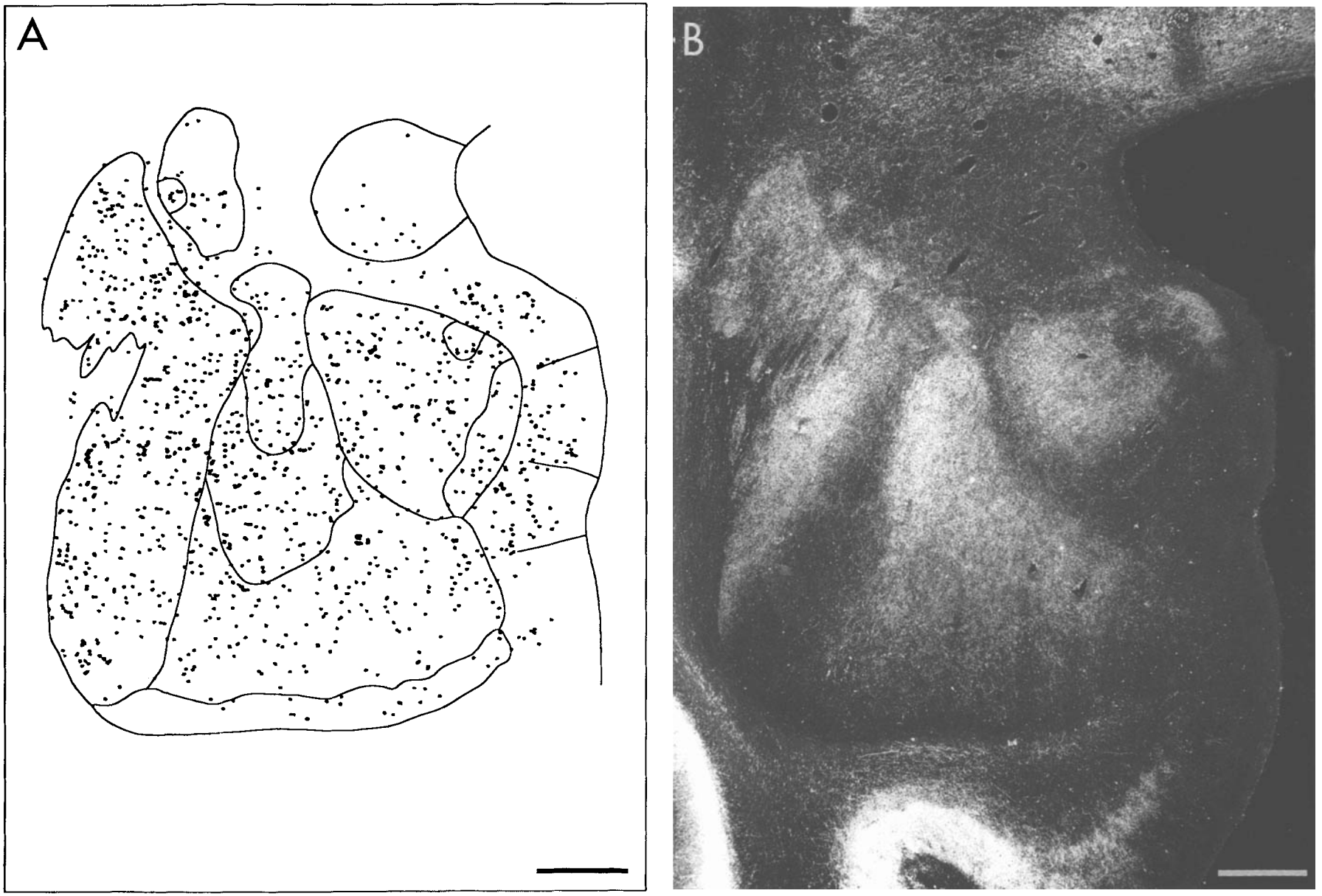

Figure 3 (See legend, p. 17)

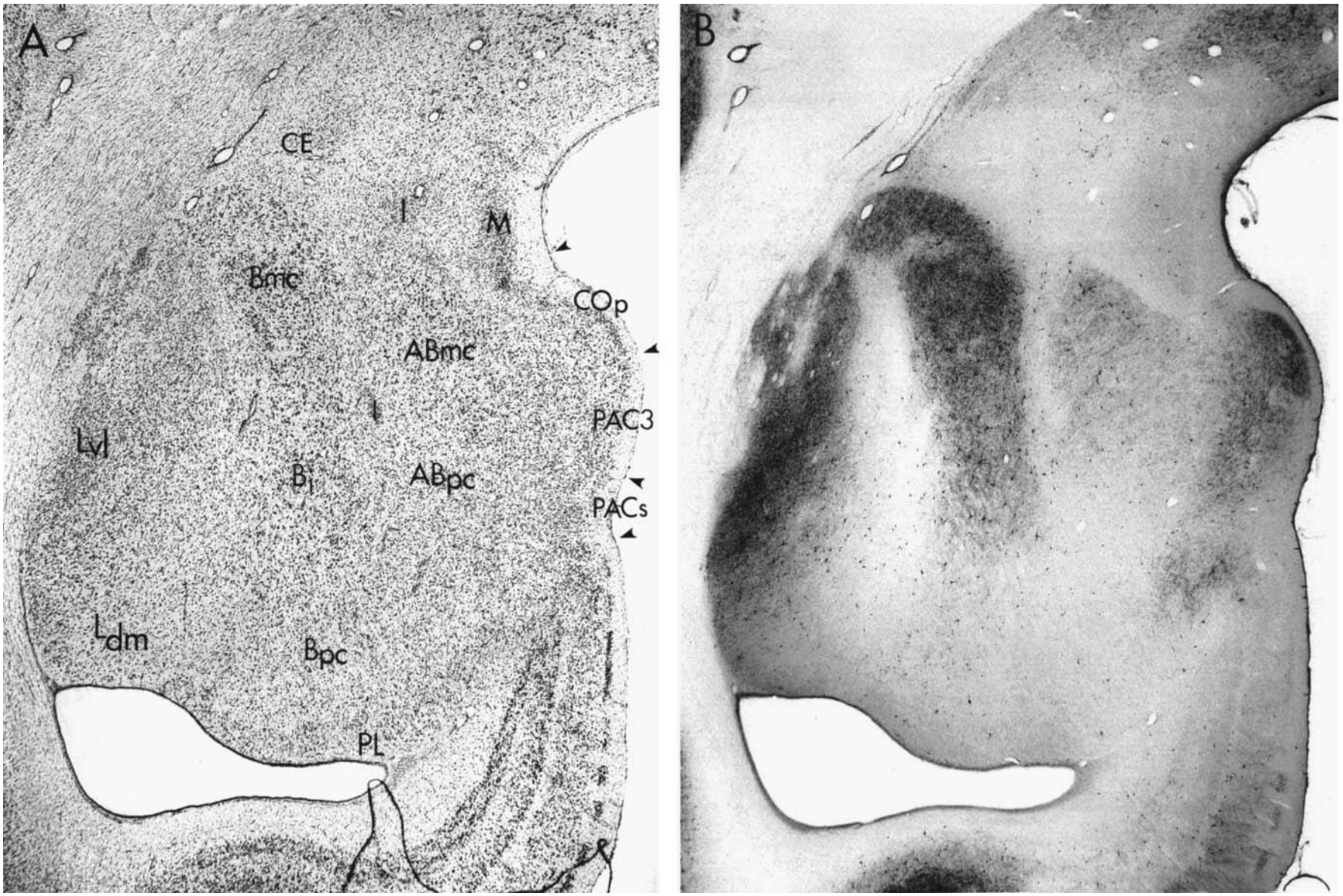

Figure 4 (See legend, p. 17)

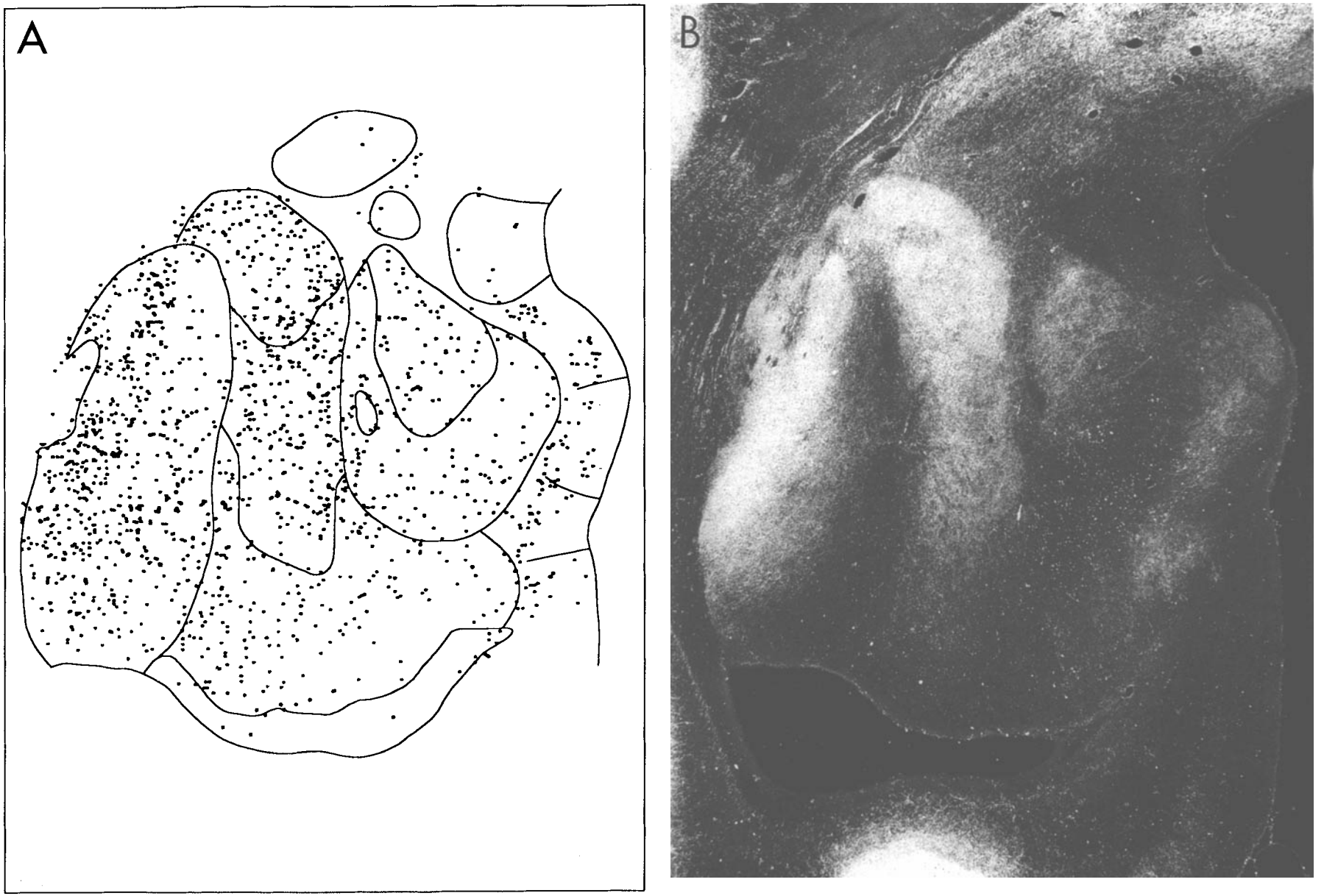

Figure 5 (See legend, p. 17)

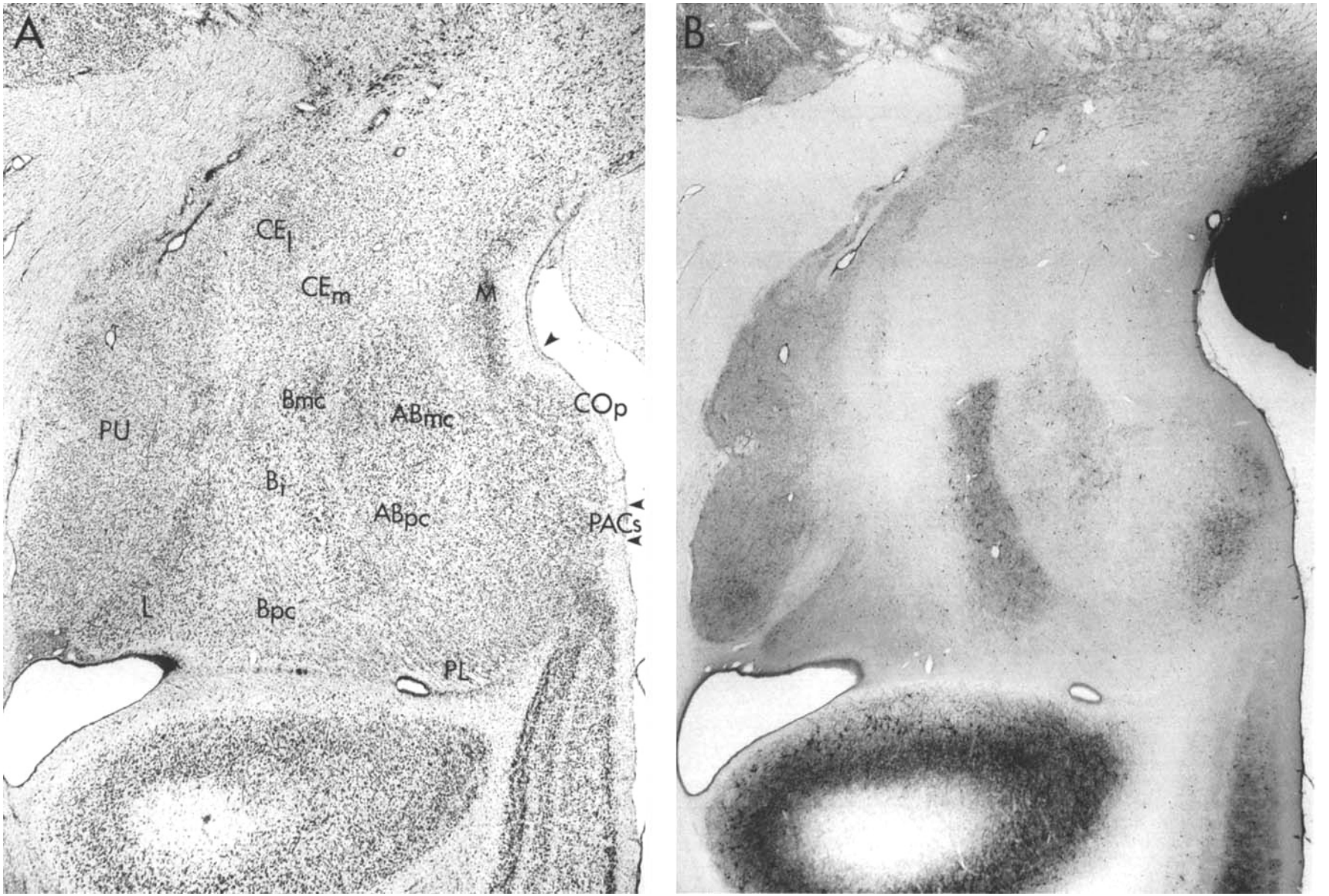

Figure 6 (See legend, p. 17)

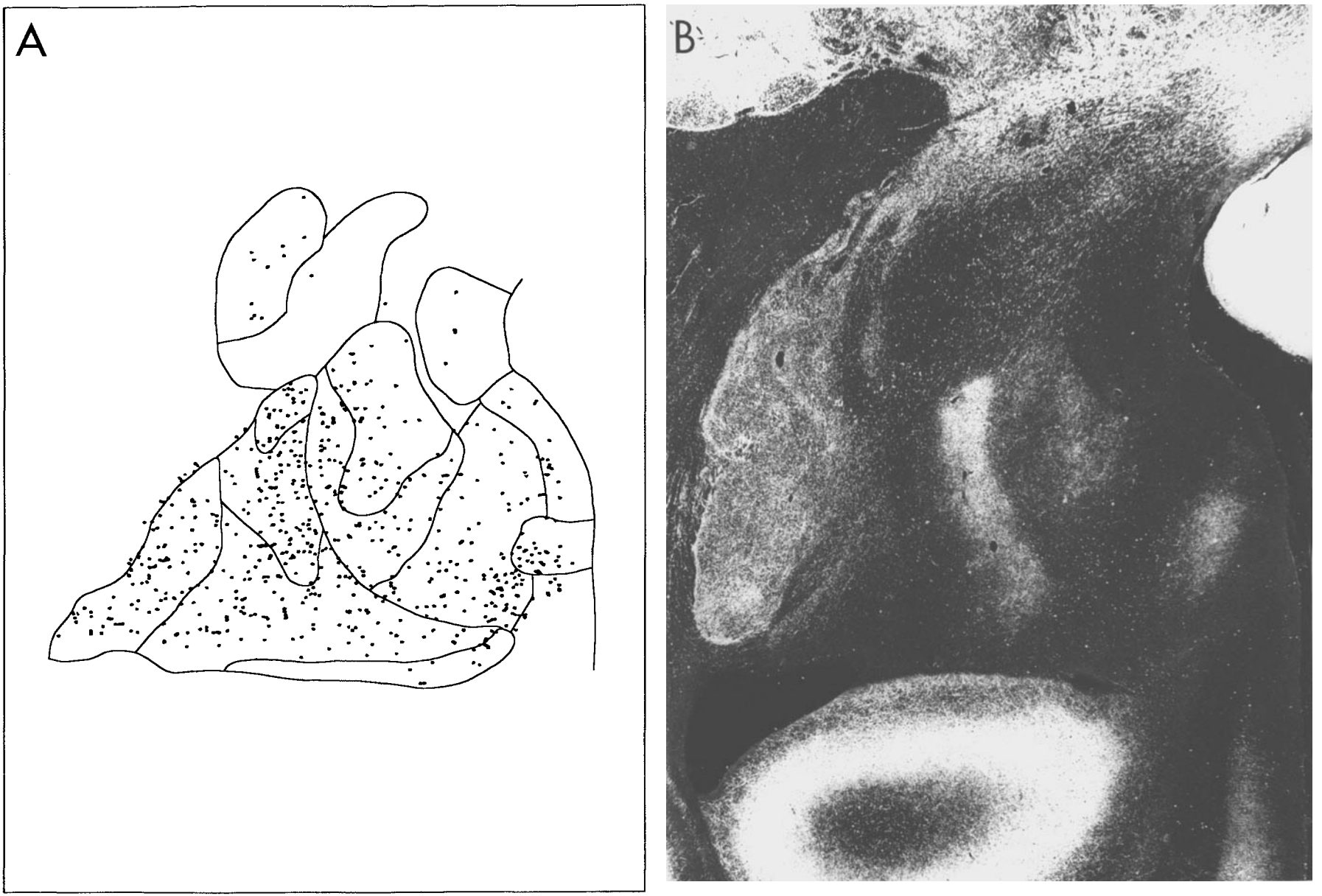

Figure 7 (See legend, p. 17)

Fig. 8. Camera lucida drawings of the three major parvalbumin-positive cell types in the amygdala. Neurons 1, 2 and 3 represent Type 1 cells, showing their variability in somal size and dendritic organization. Many of the distal dendrites of these cells demonstrated varicose dendrites (arrows). Neurons 4 and 5 illustrate two of the multipolar Type 2 cells and neuron 6 is a fusiform Type 3 cell. The somata of Type 2 and Type 3 cells are larger than those of the Type 1 cells. An axon (a) with collaterals (arrowheads) can be seen on the Type 2 cell (cell 4).

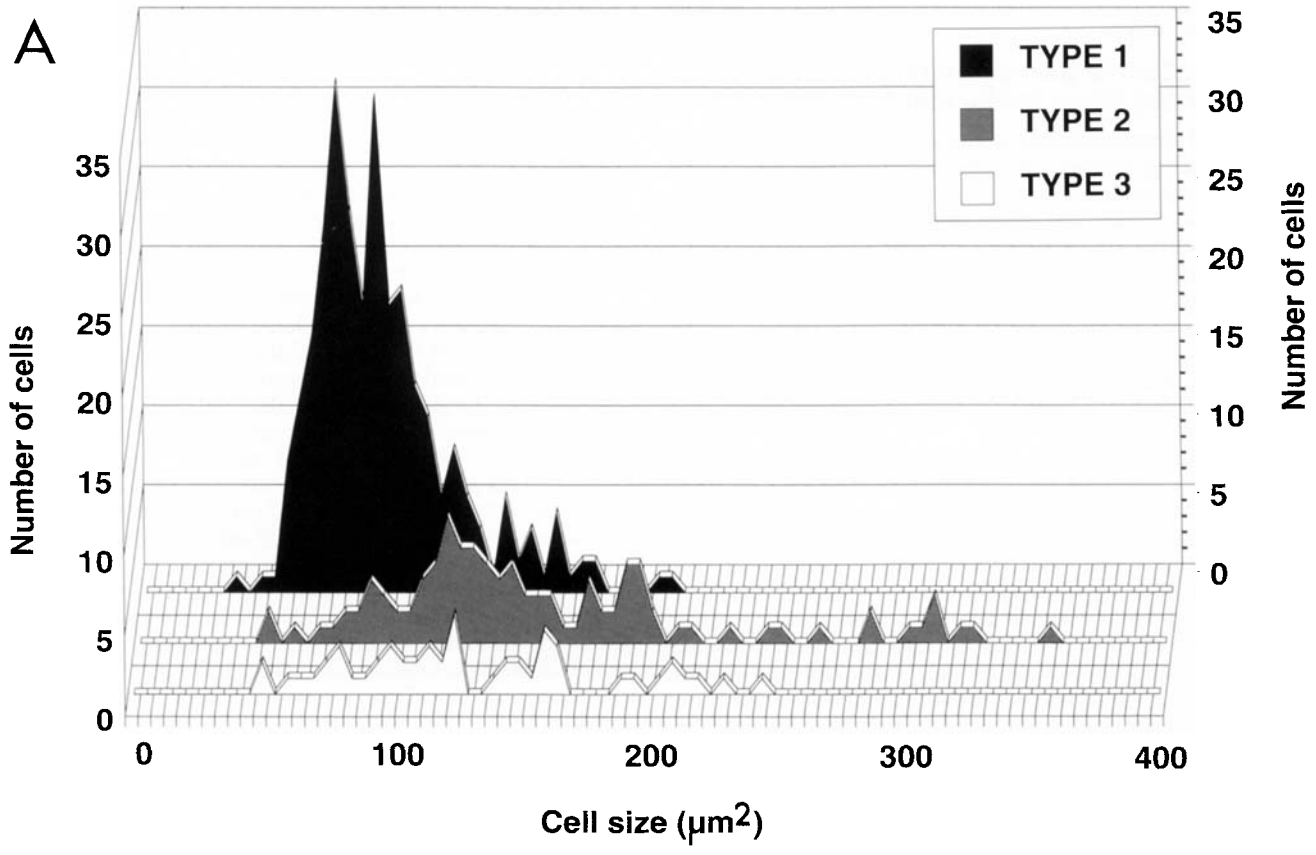

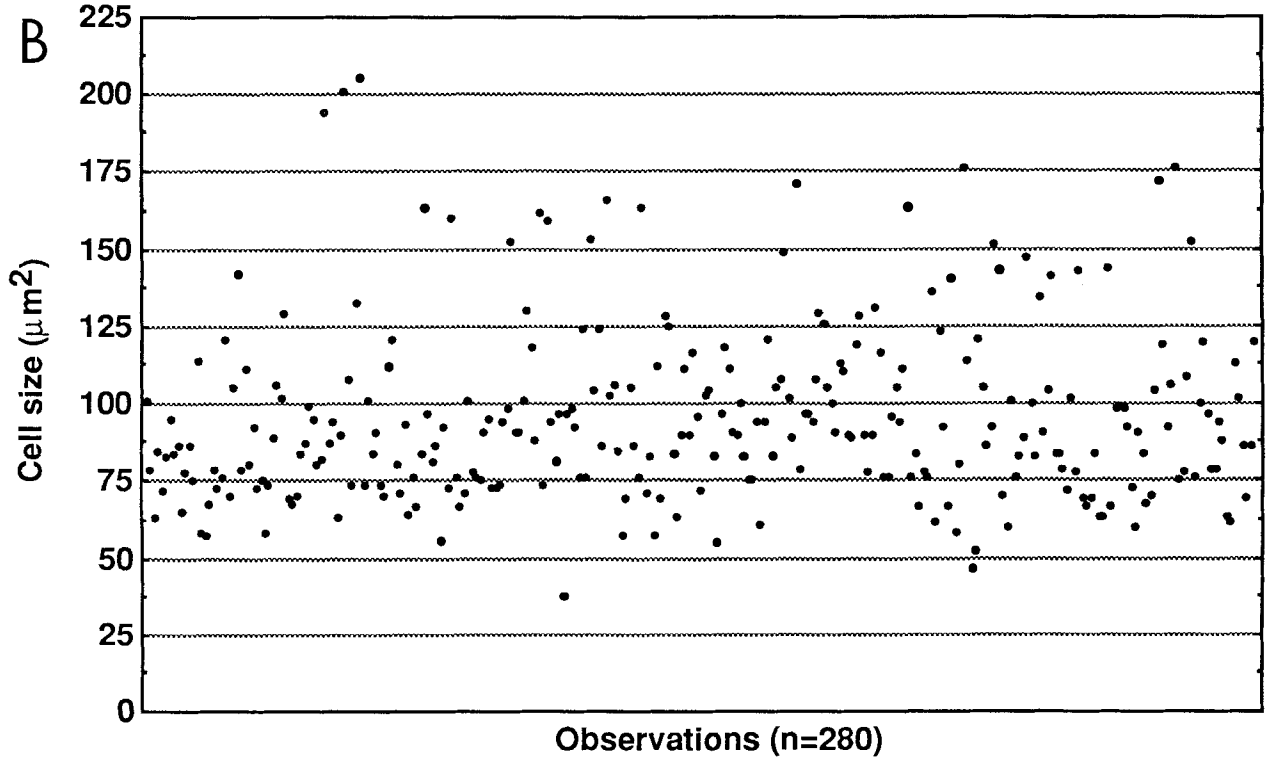

Figure 9 (See overleaf)

area (which has dorsal and ventral subdivisions), and the intercalated nuclei.

Distribution of parvalbumin-immunoreactive cells and fibers in the monkey amygdala

General characteristics of parvalbumin immunoreactivity. Before providing a detailed description of the distribution of parvalbumin-immunoreactive profiles in each of the amygdaloid nuclei and areas, we shall provide a general overview of the characteristic features of the parvalbumin staining in our preparations. The distribution and density of parvalbumin immunoreactivity in the monkey amygdala was identical in all three of the brains analyzed in this study. Parvalbumin staining consisted of immunopositive cell bodies (Figs. 8, 10–12), dendrites (sometimes stained in a Golgi-like fashion, Figs. 8, 11) and axons with varicosities (Figs. 8, 10E).

Immunopositive axons often formed basket-like plexuses around unstained somata, suggesting that at least a subpopulation of the parvalbumin cells were basket cells (Fig. 12A). These pericellular basket plexuses were seen throughout the amygdala but were most prevalent in the nucleus of the lateral olfactory tract and in the parvicellular division of the basal nucleus, where the low background staining enabled detection of even lightly labeled basket networks. Parvalbumin-immunoreactive axons also formed distinctive "cartridge" profiles (using the term of Lewis and Lund, '90) in the magnocellular and intermediate portions of the basal nucleus and in the ventrolateral division of the lateral nucleus (Fig. 12B). These cartridges consisted of linear arrays of immunoreactive varicosities (presumably presynaptic boutons) that appeared to outline the initial segments of axons of unstained neurons. These profiles resembled the cartridges that have been observed in the superficial layers of the neocortex that originate from chandelier cells (Somogyi et al., '82). We take this as suggestive evidence that at least some of the amygdaloid parvalbumin cells are likely to be chandelier cells. We also commonly observed that parvalbumin-immunoreactive axon terminals were in close apposition to the soma and proximal dendrites of other parvalbumin-immunopositive cells.

Categories of parvalbumin-immunoreactive amygdaloid neurons. All of the parvalbumin-immunoreactive cells in the monkey amygdala appeared to be aspiny or, on rare occasions, sparsely spiny. However, based on the size and shape of the labeled cell bodies and the caliber and distribution of their dendritic trees, the parvalbumin-immunopositive cells clearly formed a heterogeneous population. The population of parvalbumin-immunoreactive cells could be divided into three major cell types based primarily on the morphology of the cell body (Figs. 8, 9A, 10).

Type 1 cells were the most frequently observed and accounted for approximately 42% of the cells counted in the amygdala (Figs. 8, cells 1–3; 10A–C; Table 2). The soma of a Type 1 cell was typically spherical with many dendrites emanating from it which were of approximately equal thickness. The primary dendrites gave rise to several branches and the higher order dendritic segments typically had a beaded appearance.

The mean cross-sectional area of the Type 1 cells was 103 μm^2. This category of cell could be further divided into two subtypes based on the size and shape of the somata and the caliber of the dendrites. The more numerous population of Type 1 cells tended to be smaller and rounder with thin beaded dendrites that did not travel far from the cell body (Fig. 8, cells 1–3). The second class of Type 1 neurons consisted of cells that were somewhat larger, had more irregular somata and thicker and more darkly stained dendrites (Fig. 10C). Numerical analysis carried out on the parvalbumin-labeled cells in the lateral nucleus bore out this subdivision. The scattergram (Fig. 9B) of individual cross-sectional areas of Type 1 cells in the lateral nucleus, for example, indicates that the cross-sectional areas of most of the cells (87%) were smaller than 125 μm^2. However, the remainder of the Type 1 cells had cross-sectional areas substantially greater than this.

Type 2 cells accounted for approximately 30% of the immunopositive neurons (Table 2). The somata of Type 2 cells were angular and multipolar with at least three thick primary dendrites (Figs. 8, cells 4 and 5; 10D–F). The Type 2 cells were significantly larger than the Type 1 cells, the mean cross-sectional area of the soma being 148 μm^2. Some of these cells had long, thick and coarse dendrites (Fig. 8, cell 5). Other Type 2 cells, however, had one or two prominent main dendrites whose distal branches were thinner and beaded (Fig. 8, cell 4).

Type 3 cells accounted for approximately 14% of the counted cells (Table 2). The somata of these cells had a fusiform shape with thick dendrites emanating from the opposite poles of the soma (Figs. 8, cell 6; 10G and H). The mean cross-sectional area of the fusiform cells was 134 μm^2. About 14% of the 1,520 cells counted could not easily be assigned to any of the three categories. In most of these cases, the cells were small and did not show any visible dendrites. It is likely that at least some of these profiles

Fig. 9. (See previous page.) **A:** A histogram showing the distribution of cross-sectional areas of the three types of parvalbumin-immunoreactive cells observed in the lateral nucleus of the monkey amygdala. The histogram is based on the measurement of 516 cells drawn from one representative coronal section of the lateral nucleus. Note that there are two peaks in the distribution of Type 1 cells. Note also that the majority of the cells in the lateral nucleus are Type 1 cells and that their somal cross-sectional area is substantially smaller than the Type 2 and 3 cells. **B:** This scattergram shows the distribution of somal cross-sectional areas for Type 1 parvalbumin-immunoreactive cells (n = 280) in the lateral nucleus. Note that the sizes of most of the cells are clustered between 75 and 125 μm^2. However, there is a smaller group of cells with somal cross-sectional areas substantially above these levels. This numerical analysis confirms the qualitative observations presented in Figure 9A that Type 1 cells can be broken down into two subcategories based on somal size.

Fig. 10. Photomicrographs of parvalbumin-immunoreactive somata. **A–C:** Type 1 cells located in the lateral nucleus. The cells pictured in A and B represent the main group of Type 1 cells. These have small cell bodies and very thin and often beady dendrites. The cell in C represents the second category of Type 1 cells. The somata of these cells are somewhat larger and the dendrites are thicker than those of the cell pictured in B. **D–F:** Somata from Type 2 cells. The cell bodies are larger than those of Type 1 cells and often have an angular appearance due to the prominence of the proximal dendrites. Note the immunoreactive axon (arrows in D and E) emerging from the cell bodies of two of these neurons. The cell in D was located in the nucleus of the lateral olfactory tract, the cell in E was in the amygdalohippocampal area, and the cell in F was in the lateral nucleus. **G** and **H:** Fusiform cell bodies that make up Type 3 of the amygdaloid parvalbumin-immunoreactive cells. The cell in G was located in the parvicellular division of the basal nucleus and the one in H was located in the accessory basal nucleus. Bar in H = 10 μm and also applies to A–G.

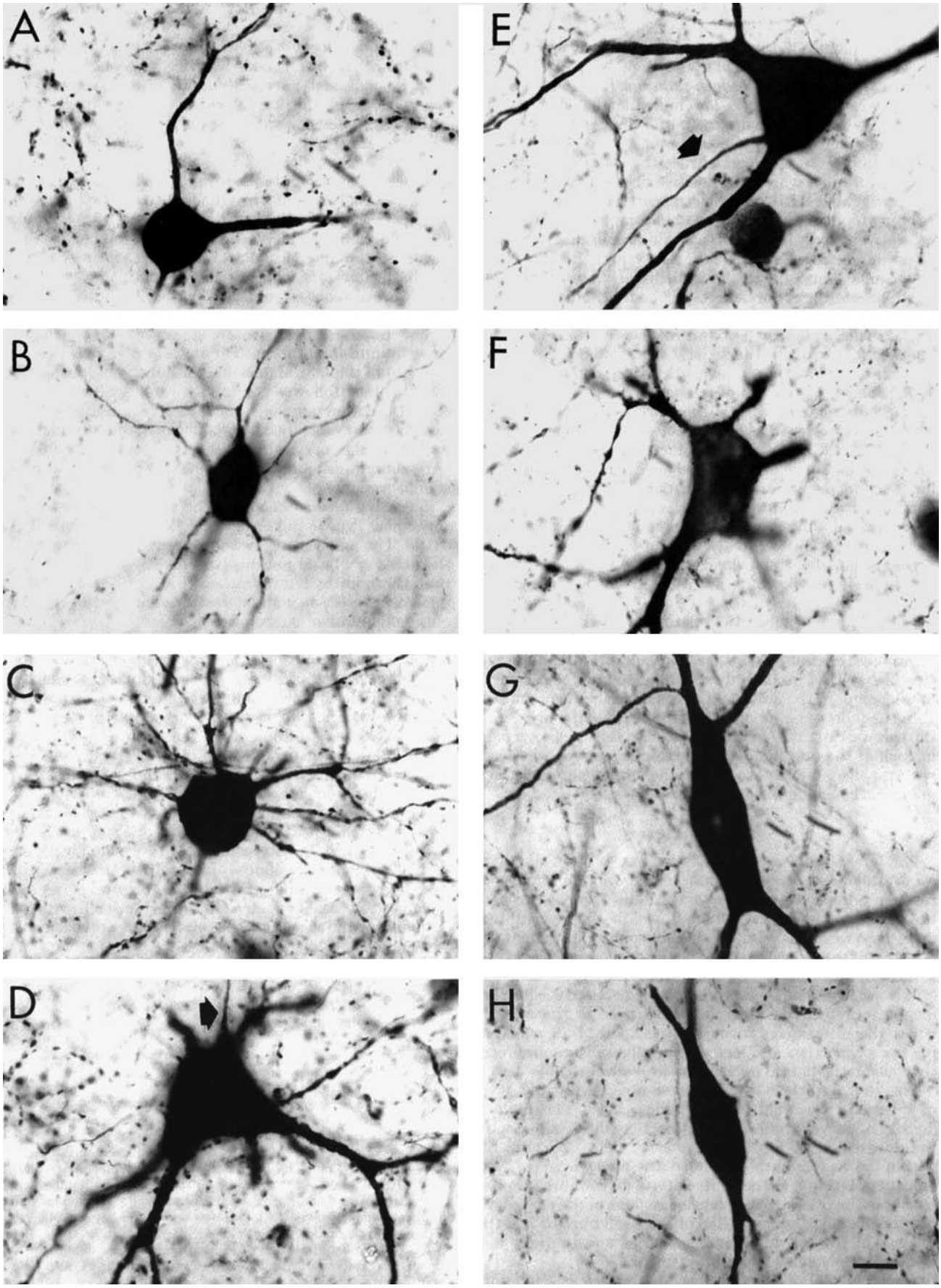

Figure 10

were fragments of parvalbumin-immunopositive neurons that were cut at the plane of the section.

Appearance of parvalbumin-immunoreactive fibers and terminals. Figure 1 is a low magnification photomicrograph showing a coronal section of a complete hemisphere of the monkey brain at a level through the amygdala. This illustration serves to demonstrate the overall pattern and density of the parvalbumin-positive fibers and terminals in the amygdala relative to adjacent cortical and subcortical regions. In general, the amygdaloid complex demonstrated a relatively low density of parvalbumin-immunoreactive fibers and terminals compared, for example, to the lateral and caudal portions of the entorhinal cortex. However, parvalbumin-immunoreactive cell bodies and fibers were not homogeneously distributed in the amygdala and in some nuclei, such as the basal nucleus or nucleus of the lateral olfactory tract, the density of stained profiles rivaled that observed in densely labeled cortical regions (Figures 1–7, Table 1). Significant differences were also found in the density of labeling within the various divisions of the amygdaloid nuclei (Figs. 2–7; Table 1). The magnocellular division of the basal nucleus, for example, had a much higher density of labeled cells and fibers than the parvicellular division. In general, the distribution and density of parvalbumin-immunoreactive cells paralleled the distribution of parvalbumin-positive fibers and terminals. The most striking exception to this was in the PAC3 division of the periamygdaloid cortex, which contained numerous parvalbumin-positive cells but had a relatively low density of parvalbumin-positive fibers.

The two major subcortical pathways of the amygdaloid complex, the ventral amygdalofugal pathway and the stria terminalis, contained very few parvalbumin-immunoreactive fibers. This would indicate that the bulk of parvalbumin labeling in the amygdala arises from intrinsic sources.

In the following sections we will describe, in more detail, the specific distribution of parvalbumin cells and terminals in each of the amygdaloid nuclei and areas. We will begin with the deep nuclei, proceed to the superficial nuclei and areas and conclude with the other amygdaloid areas.

Deep nuclei

The lateral nucleus. The lateral nucleus had the highest overall density (65 cells/mm^2) of parvalbumin-immunoreactive cell bodies in the amygdala. The Type 1 cells were the most common cell type (about 54% of all cells counted) and they were distributed quite evenly throughout all portions of the lateral nucleus. The lateral nucleus also had a substantial number of large multipolar Type 2 cells but only a few fusiform Type 3 cells. The Type 2 and 3 cells were mostly found in the ventrolateral portion of the nucleus where they intermixed with the Type 1 cells. Data concerning the proportion and size of parvalbumin-immunoreactive cells in the lateral nucleus are provided in Table 2.

The lateral nucleus demonstrated a relatively high level of fiber and terminal labeling (Figs. 2–7). The highest density of parvalbumin-immunoreactive fibers was seen in the dorsal half of the lateral nucleus (Figs. 2B and 3B) within the ventrolateral division of the nucleus. In fact, the density of labeling in the ventrolateral division was similar to that in the other densely labeled regions of the amygdala, i.e., the magnocellular division of the basal nucleus and the nucleus of the lateral olfactory tract. A substantially less dense plexus of labeled fibers and terminals was observed in the dorsomedial division of the lateral nucleus. Nonetheless, the density of parvalbumin-positive fibers in the lateral nucleus at all levels was always higher than in the medially adjacent parvicellular division of the basal nucleus. Some of the lateral capsular nuclei (Amaral and Bassett, '89) demonstrated very high densities of parvalbumin-immunoreactive fibers.

The basal nucleus. The basal nucleus had a large number of parvalbumin-positive cell bodies in its magnocellular (69 cells/mm^2) and intermediate (61 cells/mm^2) subdivisions. The parvicellular division, in contrast, had a substantially lower density (33 cells/mm^2) especially at caudal levels. In the magnocellular and intermediate divisions of the basal nucleus, Type 2 cells predominated but Type 1 cells were also observed. In the parvicellular division, Type 1 and Type 2 cells were present in about equal numbers.

The basal nucleus contained a very high density of parvalbumin-immunoreactive fibers and varicosities (Figs. 2–7). As in the lateral nucleus, the density of labeled fibers and terminals followed dorsoventral and rostrocaudal gradients. Dorsoventrally, the magnocellular and intermediate divisions had substantially greater fiber and terminal labeling than the parvicellular division and the density of parvalbumin-immunoreactive fibers decreased in a rostrocaudal gradient.

Accessory basal nucleus. The accessory basal nucleus contained Type 1 (33%), Type 2 (28%), and Type 3 cells (21%). The mean cross-sectional area of the Type 1 cells in the accessory basal nucleus was slightly higher (120 μm^2) than those in the lateral nucleus (95 μm^2). As in the basal nucleus, there was a slight rostrocaudal decreasing gradient in the number of labeled cells.

The overall density of parvalbumin-immunoreactive fiber labeling in the accessory basal nucleus was almost as high as in the lateral and basal nuclei though the density in ABmc was clearly lower than in the Bmc (Fig. 13E and F). All three portions of the accessory basal nucleus had a dense fiber plexus, although the density decreased ventrally and caudally in the parvicellular division (Figs. 2–7).

Paralaminar nucleus. The paralaminar nucleus contained only an occasional Type 1 or Type 2 cell. The density of parvalbumin-immunoreactive fibers was also very low, even lower than in the parvicellular division of the basal nucleus (Figs. 2–7). Interestingly, we occasionally observed very prominent parvalbumin-immunoreactive basket plexuses that were either entirely within the paralaminar nucleus (Fig. 12A) or straddled the border between the paralaminar nucleus and the parvicellular division of the basal nucleus.

Superficial nuclei

Nucleus of the lateral olfactory tract (NLOT). The NLOT was distinctive in having a high density of immuno-

Fig. 11. **A:** A lower magnification photomicrograph of Type 2 cells in the parvicellular division of the basal nucleus. Note that the dendrites of these cells extend for long distances and that they do not demonstrate a beady appearance. Each of the neurons on the right-hand side of the panel demonstrate a stained axon initial segment (arrows). **B:** A Type 2 cell located in the parvicellular division of the basal nucleus. Most of the dendrites in this cell have a highly varicose appearance. Arrows indicate axon initial segments. **C:** Low magnification photomicrograph of the lateral nucleus of the amygdala. A Type 2 cell is seen in the middle of the field (open arrow) with several radiating dendrites. The distal portion of at least one of these dendrites (filled arrow) has a distinctly beady appearance. There are also several spherical Type 1 cells in this field. Bars = 50 μm.

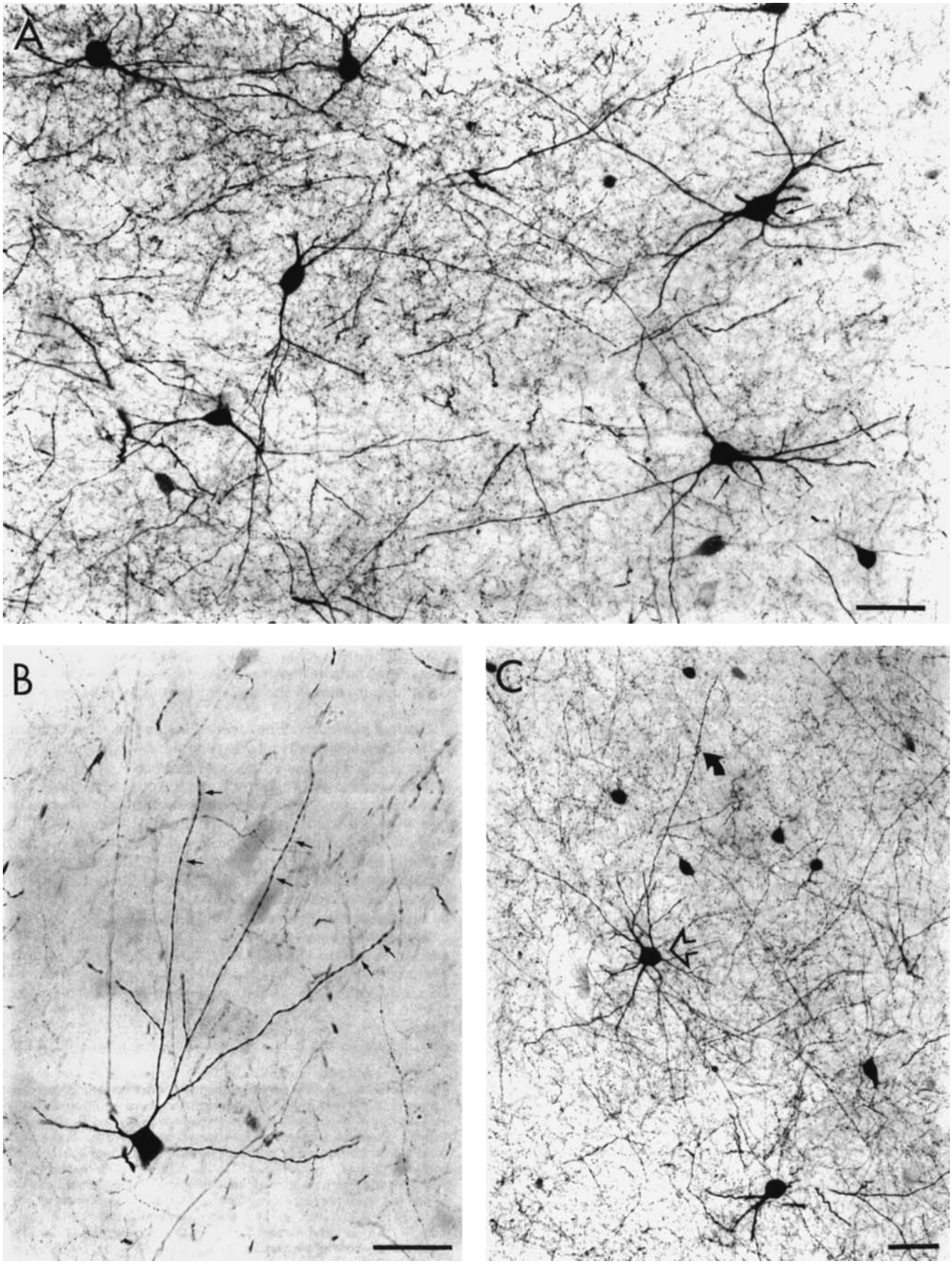

Figure 11

reactive neurons and a dense plexus of labeled fibers and terminals (Fig. 2). Numerous cells were found in layers II and III. The cells were typically the large variant (144 μm^2) of the Type 1 cells. They tended to stain darkly and their dendrites were often labeled in a Golgi-like fashion.

The NLOT had the highest density of fibers of the superficial structures (Figs. 2, 3, 13C and D). Most of the labeled fibers were associated with layer 2 where varicosities were organized in "clusters" corresponding to the darkly stained cell patches seen in Nissl-stained sections. The fibers gave rise to numerous varicosities that surrounded the unstained cells of the NLOT and formed dense pericellular baskets. The plexus of fibers continued into layer III but layer I was relatively free of parvalbumin-stained fibers.

Periamygdaloid cortex. The distribution of parvalbumin-immunoreactive cell bodies, fibers, and varicosities varied significantly in the different periamygdaloid cortical regions. Each will therefore be described separately.

PAC2. Layers II and III of PAC2 contained darkly stained Type 1 and Type 2 cells (Figs. 13A and B). There were also a number of lightly stained small cells that could not easily be assigned to one of the three major cell types because of the lack of dendritic staining.

Layer II of PAC2 had one of the highest densities of immunoreactive fibers in the amygdaloid complex and the terminal ramifications of these fibers formed conspicuous basket-like plexuses around the unstained cells (Fig. 13A and B). The cell-sparse area below layer II was devoid of parvalbumin-immunoreactive fibers. Layer III, however, did demonstrate a dense plexus of immunopositive fibers. Layer I had a relatively low number of fibers, most of which ran parallel to the pial surface.

PAC3. Layers II and III contained a relatively large number of Type 1 parvalbumin-immunoreactive cells and a few darkly stained Type 2 cells (Figs. 2–5).

The PAC3 subdivision of the periamygdaloid cortex had a lower density of parvalbumin-immunoreactive fibers than the NLOT, PAC2, or posterior cortical nucleus (compare Figs. 2–7 and 13B). However, the density of fibers in PAC3 was higher than in the sulcal portion of the periamygdaloid cortex. A loose plexus of immunoreactive fibers was found in layers II and III.

PACs. The PACs in this paper includes both PAC1 and PACs described previously (Price et al., '87). While PACs and PAC1 can be distinguished in Nissl-stained preparations, their patterns of parvalbumin immunoreactivity were not differentiable (Figs. 2–7). The parvalbumin-immunoreactive cells found in the PACs were typically small and without any visible processes; they were located mainly in layers II and III. Occasionally, a darkly stained Type 1, 2 or 3 cell was observed in the deep layers of PACs.

PACs contained a low density of parvalbumin-labeled fibers, which were located mainly in layers II and III. Often the fibers seemed to run perpendicularly from the deep layers to reach the more superficial portion of PACs. In some sections, an immunopositive fiber bundle that was situated between the parvicellular division of the basal nucleus and the entorhinal cortex appeared to turn medially to enter the PACs. PACs had a significantly lower density of fibers than the ventrally adjacent olfactory region of the entorhinal cortex.

Anterior cortical nucleus. The anterior cortical nucleus contained only a few parvalbumin-immunoreactive cells, which were generally small and did not have any visible dendritic processes (Figs. 2 and 3). Most of the cells were in the deep part of layer II. There was also a very low level of parvalbumin-immunoreactive fibers in the anterior cortical nucleus; an occasional labeled fiber was observed in layer II.

Medial nucleus. At rostral levels, the medial nucleus demonstrated only an occasional lightly stained parvalbumin-immunoreactive cell with no visible dendrites located either in layer II or layer III (Figs. 4–7). In the caudal half of the nucleus, there was a cluster of small parvalbumin-positive cells in layers II and III. As in the anterior cortical nucleus, the medial nucleus had a very low density of parvalbumin-labeled fibers and terminals. Only an occasional immunopositive fiber was found in layers I and II.

Posterior cortical nucleus. The posterior cortical nucleus contained a somewhat higher density of parvalbumin-immunoreactive profiles than the anterior cortical or medial nuclei (Figs. 4–7). Most of the parvalbumin-immunoreactive cells were located rostrally in layer II and belonged to the Type 1 or Type 2 category. Caudally, only an occasional lightly stained cell was found.

Rostrally, the posterior cortical nucleus contained a relatively dense plexus of parvalbumin-immunoreactive fibers that formed basket-like plexuses around the unstained cells. This pattern of labeling resembled that observed in PAC2 and NLOT. At more caudal levels, a dense plexus was observed in the ventral portion of the posterior cortical nucleus, though this plexus decreased in density such that at the most caudal levels the nucleus was almost empty of parvalbumin-immunoreactive fibers.

Other nuclei

Anterior amygdaloid area. There were several Type 1 cells in the anterior amygdaloid area (Fig. 3A). The density of parvalbumin-immunoreactive fibers was low but somewhat higher than in the anterior cortical, medial or central nuclei.

Central nucleus. The central nucleus was distinguished by its extremely low level of parvalbumin immunoreactivity (Figs. 4–7). The few immunoreactive cells that were observed were lightly stained small cells with no visible dendrites. The density of parvalbumin-immunoreactive fibers and varicosities was perhaps the lowest in the amygdaloid complex. The lateral division of the central nucleus had no visible immunopositive fibers. The medial division demonstrated a low number of fibers that did not appear to form terminal plexuses. Certainly no pericellular baskets were observed in this nucleus.

Amygdalohippocampal area. The density of labeled cells and fibers varied substantially in different portions of the amygdalohippocampal area. Anterior and dorsal portions of the amygdalohippocampal area had only an occasional

Fig. 12. **A:** In the center of the field are three dense parvalbumin-immunoreactive basket plexuses (open arrows) with several preterminal axons. A parvalbumin-immunoreactive cell body is located near the baskets but it is not clear whether this cell gives rise to the labeled baskets. The basket plexuses are located at the border between the paralaminar nucleus and the lateral nucleus. Additional lightly labeled baskets (filled arrows) are visible in the top half of the panel. **B:** Low magnification brightfield photomicrograph of the magnocellular division of the basal nucleus, using Nomarski optics. The numerous linear profiles (some of which are indicated with arrows) are "cartridges" of parvalbumin-immunoreactive terminals that appear to line the initial segments of axons of unstained basal nucleus neurons. Bar in A = 50 μm; B = 20 μm.

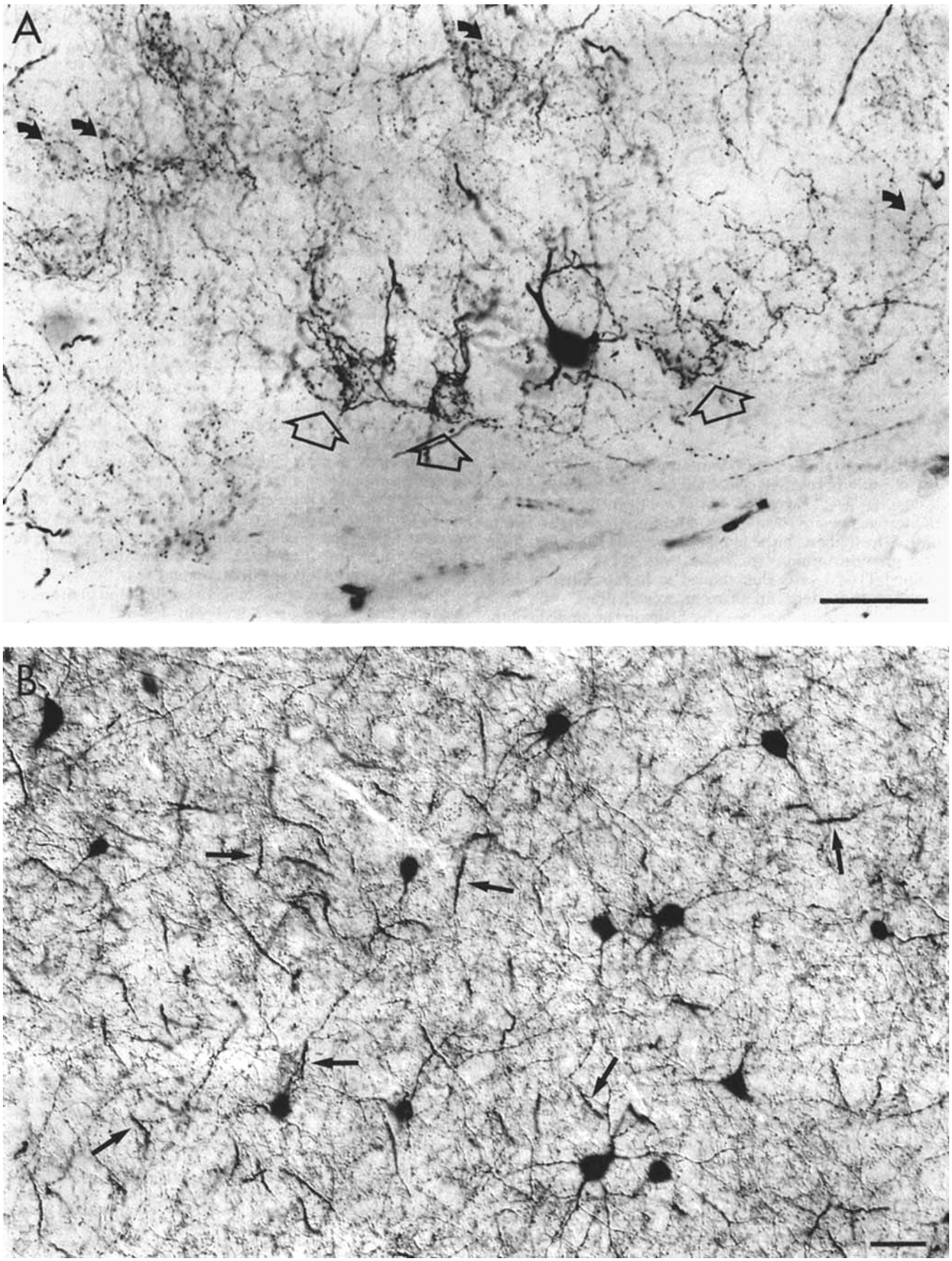

Figure 12

TABLE 1. Density of Parvalbumin-Immunoreactive Cells and Fibers in the Amygdala

Amygdaloid area	Subdivision	Cells	Fibers
Lateral nucleus		+++	+++
Basal nucleus	magnocellular	+++	+++
	intermediate	+++	+++
	parvicellular	+	+
Accessory basal nucleus	magnocellular	++	++
	parvicellular	++	++
	ventromedial	++	++
Paralaminar nucleus		+	+
Anterior cortical nucleus		+	+
Medial nucleus		+	(+)
Posterior cortical nucleus		+	+
Amygdalohippocampal area		++	++
PAC2		++	+++
PAC3		++	+
PACs		++	+
Nucleus of the lateral olfactory tract		+++	+++
Central nucleus	medial	(+)	+
	lateral	(+)	(+)
Anterior amygdaloid area		++	+
Intercalated nuclei		++ or −	++ or −

Abbreviations: the number of cells and the density of fibers are expressed as +++ high, ++ medium, + low, (+) occasionally found, − not found.

small, lightly stained parvalbumin-positive cell. The number of immunoreactive cells increased markedly at caudal levels, however, especially in the ventromedial portion of the nucleus where the density of immunoreactive cells was one of the highest in the monkey amygdala (63 cells/mm^2). The greatest number of these cells (54%) were darkly stained Type 1 cells that tended to have relatively small somal cross-sectional areas (mean area 88 μm^2).

Parvalbumin-immunoreactive fibers in the amygdalohippocampal area were located mostly in the ventral half of the region especially at rostral levels. While the fiber staining was fairly dense in these regions, the labeling did not completely occupy all of the ventral region of the AHA as defined by Pitkänen and Amaral ('91).

Intercalated nuclei. The density of parvalbumin-immunoreactive cells and fibers varied from one intercalated nucleus to another. In some intercalated nuclei, there were numerous darkly stained Type 1 cells with very short, if any, visible dendritic processes (Fig. 13G and H). In these nuclei, there was also a very high density of immunoreactive fibers. In other intercalated nuclei, however, such as those typically found between the magnocellular division of the basal nucleus and the lateral nucleus or between the basal and accessory basal nuclei, there was virtually no parvalbumin immunoreactivity (Figs. 4 and 5).

DISCUSSION

We have presented a description of the distribution of parvalbumin-immunoreactive cell bodies, fibers and terminals in the various nuclei and cortical regions of the monkey amygdaloid complex. Certain nuclei of the monkey amygdala contained numerous parvalbumin-immunoreactive cell bodies and a dense plexus of parvalbumin-immunoreactive fibers and terminals. Overall, however, the density of parvalbumin immunoreactivity in the amygdala was substantially lower than in the surrounding cortical and subcortical regions. The distribution of parvalbumin-immunoreactive cells and fibers was often found to respect the cytoarchitectonic boundaries of the different amygdaloid nuclei. Most of the parvalbumin immunoreactivity was located in the deep nuclei of the amygdala. Extremely low levels of parvalbumin immunoreactivity was observed in certain areas such as the central and medial nuclei, both of which are known to be rich in various types of neuropeptide-containing cells and fibers. The parvalbumin-immunoreactive cells observed in the amygdala are a morphologically heterogeneous group of aspiny neurons. The parvalbumin-immunoreactive fibers in the amygdala commonly formed pericellular baskets around unstained cell bodies and, in some regions such as the magnocellular division of the basal nucleus, also formed "cartridges" of terminals along the initial axon segments of unstained neurons. It would appear, therefore, that many of the immunopositive neurons in the amygdala are similar to the basket and chandelier cell types that demonstrate parvalbumin immunoreactivity in the neocortex.

Parvalbumin-immunopositive cells in the monkey amygdaloid complex

All of the parvalbumin-immunoreactive cells found in the monkey amygdaloid complex were aspiny nonpyramidal cells. They ranged in size and shape from small round neurons with thin beaded dendrites to large multipolar cells with thick long dendrites. Although the dendrites of some parvalbumin-positive neurons extended several hundred microns from the soma, the dendritic trees mostly remained within the same nucleus as the parent soma. Most of the labeled neurons resembled cells, which in Golgi studies of the amygdaloid complex, are considered to be intrinsic neurons (McDonald, '82; Braak and Braak, '83; Millhouse and DeOlmos, '83; McDonald, '84).

The parvalbumin-immunoreactive cells found in the monkey amygdaloid complex could be divided into three major morphological classes based on somal size and shape and the size and distribution of their dendrites. Type 1, which were the most frequent, had round or oval somata with 3 to 12 thin dendrites giving them a multipolar appearance. We differentiated two subclasses of Type 1 cells based primarily on the size of the cell soma and the thickness of dendrites. It will be of interest to determine whether the different Type 1 cells can also be differentiated on the basis of the other neuroactive substances they may contain or by their patterns of connectivity. The Type 1 cells (Figs. 8, cells 1–3; 10A and C) resembled the smaller aspiny or sparsely spiny Class III cells, which are devoid of lipofuscin granules, illustrated in the Golgi material of Braak and Braak (Fig. 8, cells d,e and h of Braak and Braak, '83) from the human amygdala or the small multipolar class II cells pictured by MacDonald (Fig. 7, cell e and Fig. 11 of McDonald, '82) from Golgi studies of the rat basolateral nucleus of the amygdala.

Fig. 13. Nissl (left side) and parvalbumin immunohistochemical (right side) sections through various regions of the monkey amygdala. **A** and **B:** The PAC2 division of the periamygdaloid cortex. Note the dense fiber and terminal labeling in layer II. **C** and **D:** The nucleus of the lateral olfactory tract is shown at the surface of the amygdala on the left side of the panel. The fiber and terminal labeling in the NLOT is among the heaviest in the amygdaloid complex. Scattered cells are observed in the ventral portion of the nucleus. **E** and **F:** The border between the dorsal portions of the accessory basal nucleus and the magnocellular division of the basal nucleus is illustrated in these panels. Note the much denser fiber and terminal labeling in the magnocellular division of the basal nucleus. **G** and **H:** An intercalated nucleus located ventral to the anterior amygdaloid area (AAA). In this particular intercalated nucleus, there is relatively low fiber and terminal labeling. There are a small number of Type 1 parvalbumin-immunoreactive neurons within the nucleus. Bars: A–F, 200 μm; G and H, 50 μm.

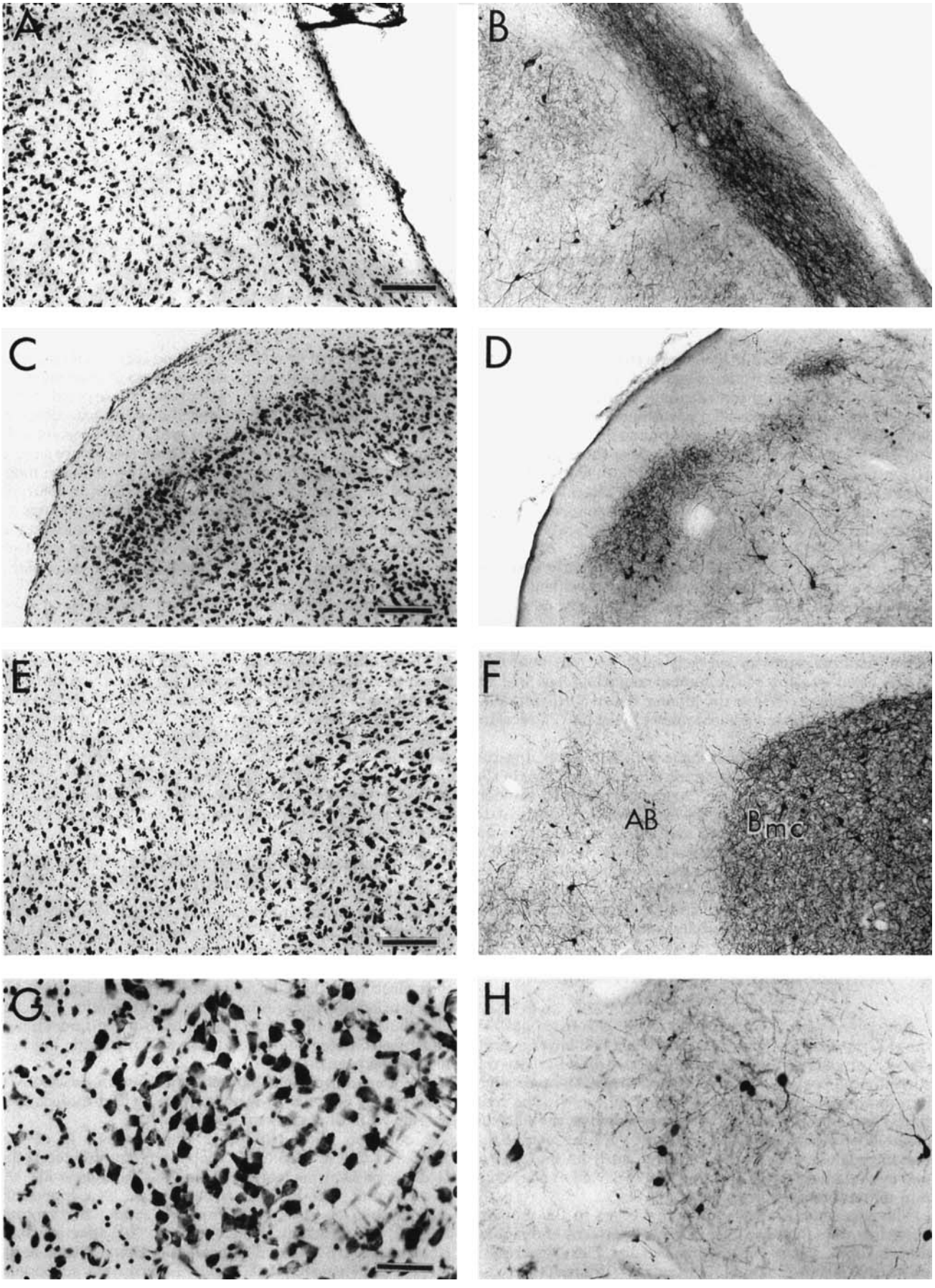

Figure 13

TABLE 2. The Number and Size of Parvalbumin-Immunoreactive Cell Types in the Monkey Amygdala[1]

Area	Cell type	Cell number	% of cells	Cells/ mm²	Mean size ± SD (μm²)	Minimum[3] (μm²)	Maximum[3] (μm²)
ALL[2]	All types	1,520	100	45	120 ± 51	23	402
	Type 1	647	42	19	103 ± 36*** ###	23	304
	Type 2	450	30	13	148 ± 57##	44	397
	Type 3	211	14	6	134 ± 55	43	402
	Unclassified	212	14	6	100 ± 39	25	242
Lateral ncl.	All types	516	100	65	111 ± 49	25	357
	Type 1	280	54	35	95 ± 28*** ###	38	205
	Type 2	110	21	14	158 ± 64#	53	357
	Type 3	53	11	7	133 ± 49	52	247
	Unclassified	73	14	9	86 ± 30	25	218

[1]The data are shown for all counted cells as well as for cells located in the lateral nucleus.
[2]ALL refers to all cells counted in the lateral nucleus, basal nucleus, accessory basal nucleus, nucleus of the lateral olfactory tract, PAC2, PAC3, PACs, and amygdalohippocampal area.
[3]Minimum and maximum refer to the smallest and largest cell areas found in the specified region.
Statistical significances: ***P < 0.001 compared to Type 2 cells; ###P < 0.001; ##P < 0.000; #P < 0.05 compared to Type 3 cells.

Type 2 were larger multipolar cells that were particularly prominent in the ventrolateral part of the lateral nucleus, the magnocellular and intermediate portions of the basal nucleus, the accessory basal nucleus and in the NLOT. The large Type 2 cells with thick and coarse dendrites (Figs. 8, cell 5; 10E) resembled the larger forms of the Braak's Class III or nonpigmented aspiny neurons (see Fig. 9a and b, Braak and Braak, '83) described in the lateral nucleus of the human amygdala. Our Type II cells also resembled the multipolar class II neurons of the rat basolateral amygdala described by McDonald (see Fig. 7D, McDonald, '82).

The fusiform Type 3 cells were less frequently observed than the first two cell types and were most prevalent within the deep nuclei. Interestingly, the morphology and dimensions of the soma and dendritic tree of the Type 3 cells (Figs. 8, cell 6; 10G and H) were similar to the Class II pigment-laden fusiform aspiny or sparsely spiny neurons described in the basal nucleus of the human amygdala (see Fig. 8f, Braak and Braak, '83) or the bipolar class II cells found in the rat basolateral amygdaloid nucleus (see Fig. 7f, McDonald, '82).

There has been relatively little written concerning the distribution of parvalbumin-immunoreactive profiles in the amygdala. Celio ('90) found "large neurons with slender, spineless cell processes" in the basolateral (equivalent to the basal nucleus in monkey) and lateral nuclei of the rat amygdala. While the illustration of these immunoreactive neurons (Fig. 21 of Celio, '90) indicates that there may be some variability in the size and shape of parvalbumin-immunoreactive neurons in the rat amygdala, it is not possible to compare these cells with the ones we have observed in the monkey.

Parvalbumin-immunoreactive fibers in the amygdala

Consistent with the findings of Celio ('90) from work in the rat, the monkey amygdaloid complex had lower overall density of parvalbumin-immunoreactive fibers than the surrounding cortical regions. Interestingly, the parvalbumin-immunoreactive fibers were mostly located in the deep nuclei and a few superficial structures such as the nucleus of the lateral olfactory tract and the PAC2 division of the periamygdaloid cortex. Other nuclei, such as the central and medial nuclei, were almost entirely devoid of parvalbumin-immunoreactive cells and fibers.

The parvalbumin-immunoreactive fibers in the monkey amygdala were found to form different patterns of terminal arborizations. These included basket-like plexuses around unstained somata, axonal "cartridges" around the axon initial segments of unstained cells, and individual terminals in apposition to the dendritic tree or soma of unstained and parvalbumin-immunoreactive neurons. These profiles were in addition to a more diffuse distribution of parvalbumin-immunoreactive varicosities for which the postsynaptic element could not be determined. These results are suggestive that the parvalbumin-immunoreactive cells are members of at least two subclasses of GABAergic neurons, namely, basket cells and chandelier cells. These findings are consistent with observations in the monkey and human neocortex where parvalbumin immunoreactivity has been clearly associated with basket and chandelier cells (DeFelipe et al., '89; Blümcke et al., '90; Lewis and Lund, '90). Interestingly, MacDonald ('82) had previously demonstrated chandelier cells in the basal nucleus of the rat amygdala with the Golgi technique.

The origins of the parvalbumin fibers providing the dense plexuses in the amygdala are not known. Since all of the parvalbumin-immunoreactive cells in the amygdala were aspiny and therefore likely to be intrinsic interneurons (McDonald, '82; Braak and Braak, '83; Millhouse and DeOlmos, '83) much of the parvalbumin fiber system is probably generated locally. This conclusion is also supported by the fact that there were few, if any, parvalbumin-immunoreactive fibers in the stria terminalis or ventral amygdalofugal pathway.

Colocalization of parvalbumin with other neuroactive substances

Relatively limited information is available concerning the chemoarchitecture of the primate amygdaloid complex (Amaral et al., '92). Comparing the results of the present study to the published literature pertaining to the primate brain, it is clear that there is no tight correlation between the distribution of parvalbumin immunoreactivity and the distribution of other neurotransmitter or neuromodulator substances. Since the distribution of GABAergic markers has not yet been described in the monkey, however, and this is the transmitter that parvalbumin immunoreactivity is most tightly linked to, it is not surprising that there is little overlap with other transmitter candidates.

A common finding in other brain regions in several species, including monkey, is that parvalbumin is located in GABAergic neurons (cortex: Celio, '86; Defelipe et al., '89; Hendry et al., '89; Demeulemeester et al., '91a; hippocampus: Kosaka et al., '87; Katsumaru et al., '88; septum: Freund, '89; striatum: Waldvogel et al., '91; olfactory bulb: Kosaka et al., '87; lateral geniculate nucleus: Stichel et al., '88; Demeulemeester et al., '91b). Moreover, the subpopula-

tion of GABAergic cells that is immunoreactive for parvalbumin is different from the population of GABAergic cells immunoreactive for somatostatin (Nitsch et al., '90), neuropeptide Y (Nitsch and Leranth, '91) or cholecystokinin (Katsumaru et al., '88; Gulyas et al., '91). Recently, McDonald and Baimbridge ('90) reported that virtually all parvalbumin-immunoreactive neurons in the rat basolateral amygdala also contain GABA. Interestingly, in the rat amygdala a high density of GABA-immunoreactive cell bodies was found in the lateral, basolateral, and cortical nuclei and many fewer cells were found in the central and medial nuclei (McDonald, '85; Ottersen et al., '86; Nitecka and Ben-Ari, '87). The distribution of the GABA-immunoreactive cell bodies in the rat amygdala would appear to parallel, therefore, the distribution of parvalbumin-immunoreactive cell bodies in the monkey amygdaloid complex. The pattern of GABAergic fiber and terminal labeling in the rat amygdala, however, is not entirely consistent with the pattern of parvalbumin immunoreactivity we have seen in the monkey. Ottersen et al. ('86) and Nitecka and Ben-Ari ('87), for example, reported a dense GABAergic innervation of the central and medial nuclei, which are both almost devoid of parvalbumin-immunoreactive terminal labeling. A much lower level of GABAergic neuropil staining was reported in the lateral, basal, and cortical nuclei of the rat amygdaloid complex. As we have noted, these nuclei have a dense parvalbumin-immunoreactive fiber and terminal plexus. The differences in the pattern of terminal labeling between GABA and parvalbumin immunoreactivities may reflect the fact that parvalbumin is located only in a subpopulation of the GABAergic neurons. The extent of colocalization of GABA and parvalbumin in the monkey amygdaloid complex awaits further study.

As noted above, parvalbumin-immunoreactive cells in other brain regions typically do not colocalize with peptides. In the amygdala, a comparison of the distribution of peptide and parvalbumin-immunoreactive profiles appears consistent with this finding. In the basal nucleus, for example, there is a relatively low density of somatostatin-immunoreactive cell bodies (Amaral et al., '89) but numerous parvalbumin-positive neurons. Conversely, in the lateral portion of the central nucleus, there are numerous somatostatin-immunoreactive cell bodies but almost no parvalbumin-immunoreactive neurons. Similarly, neuropeptide Y immunopositive cell bodies were found to be rare in the accessory basal nucleus (Smith et al., '85), which had a large number of parvalbumin-positive neurons. Thus, available evidence would suggest that few, if any, of the parvalbumin-immunoreactive neurons will also contain peptide transmitter candidates.

We have recently analyzed the distribution of the enzyme NADPH-diaphorase (NADPH-d) in the monkey amygdala. The stellate-like NADPH-d positive cells (Fig. 3d–f, Pitkänen and Amaral, '91) as well as the large multipolar NADPH-d cells (Fig. 3a, Pitkänen and Amaral, '91) share morphological similarities with some of the Type 1 (Fig. 10A–C) and Type 2 (Fig. 10E) parvalbumin-immunoreactive cells, respectively. The density of both NADPH-diaphorase-positive and parvalbumin-immunoreactive fibers was high in the ventrolateral portion of the lateral nucleus, in the accessory basal nucleus, and in the NLOT and low in the central, medial, and anterior cortical nuclei. The most striking differences in the terminal labeling between NADPH-d and parvalbumin immunoreactivity were seen in the magnocellular and intermediate divisions of the basal nucleus and in PAC2, where we observed a dense plexus of parvalbumin-immunoreactive terminals but very low NADPH-d fiber and terminal staining (Pitkänen and Amaral, '91).

In the dorsal portion of the lateral geniculate nucleus of the cat (Demeulemeester et al., '91), the dorsal root ganglia of rat (Carr et al., '89), and in the human cerebellum (Kobayashi et al., '90), parvalbumin was found to colocalize with another calcium-binding protein, calbindin-D_{28k}. In the monkey neocortex and hippocampus, however, these two calcium-binding proteins seem to be located in different cell populations (Van Brederode et al., '90; Seress et al., '91). While McDonald and Baimbridge ('90) reported substantial colocalization of parvalbumin with calbindin in the basolateral nucleus of the rat amygdala, our own preliminary studies indicate that the distribution of these two calcium-binding proteins are quite different in the monkey amygdala (Pitkänen and Amaral, unpublished observations).

ACKNOWLEDGMENTS

This work was supported by NIMH grant MH41479 (to D.G. Amaral), by a Fogarty International Fellowship (1 F05 TW04343) and by the Academy of Finland, Medical Council (to A. Pitkänen). This work was also conducted, in part, at the California Regional Primate Center in Davis, CA, NIH Grant (RR00169). We thank Mary Ann Lawrence for histological assistance, Kris Trulock for photographic processing, and Belle Wamsley for secretarial assistance.

LITERATURE CITED

Amaral, D.G., and J.L. Bassett (1989) Cholinergic innervation of the monkey amygdala: An immunohistochemical analysis with antisera to choline acetyltransferase. J. Comp. Neurol. *281:*337–361.

Amaral, D.G., C. Avendaño, and R. Benoit (1989) Distribution of somatostatin-like immunoreactivity in the monkey amygdala. J. Comp. Neurol. *282:*294–313.

Amaral, D.G., J.L. Price, A. Pitkänen, and S.T. Carmichael (1992) Anatomical organization of the primate amygdaloid complex. In J. Aggleton (ed): The Amygdala. New York: Wiley-Liss Publishers, 1–66.

Berod, A., B.K. Hartman, and J.F. Pujol (1981) Importance of fixation in immunohistochemistry: Use of formaldehyde solutions at variable pH for the localization of tyrosine hydroxylase. J. Histochem. Cytochem. *29:*844–850.

Blümcke, I., P.R. Hof, J.H. Morrison, and M.R. Celio (1990) Distribution of parvalbumin immunoreactivity in the visual cortex of old world monkeys and humans. J. Comp. Neurol. *301:*417–432.

Braak, H., and E. Braak (1983) Neuronal types in the basolateral amygdaloid nuclei of man. Brain Res. Bull. *11:*349–365.

Carr, P.A., T. Yamamoto, G. Karmy, K.G. Baimbridge, and J.I. Nagy (1989) Parvalbumin is highly colocalized with calbindin D28k and rarely with calcitonin gene-related peptide in dorsal root ganglia neurons of rat. Brain Res. *497:*163–170.

Celio, M.R. (1986) Parvalbumin in most γ-aminobutyric acid-containing neurons of the rat cerebral cortex. Science *231:*995–997.

Celio, M.R. (1990) Calbindin D-28k and parvalbumin in the rat nervous system. Neuroscience *35:*375–475.

Celio, M.R., W. Baier, L. Schärer, P.A. De Viragh, and C.H. Gerday (1988) Monoclonal antibodies directed against the calcium binding protein parvalbumin. Cell Calcium *9:*81–88.

Cowan, R.L., C.J. Wilson, P.C. Emson, and C.W. Heizmann (1990) Parvalbumin-containing GABAergic interneurons in the rat neostriatum. J. Comp. Neurol. *302:*197–205.

DeFelipe, J., S.H.C. Hendry, and E.G. Jones (1989) Visualization of chandelier cell axons by parvalbumin immunoreactivity in monkey cerebral cortex. Proc. Natl. Acad. Sci. USA *86:*2093–2097.

Demeulemeester, H., L. Arckens, F. Vandesande, G.A. Orban, C.W. Heizmann, and R. Pochet (1991a) Calcium binding proteins and neuropep-

tides as molecular markers of GABAergic interneurons in the cat visual cortex. Exp. Brain Res. *84:*538–544.

Demeulemeester, H., L. Arckens, F. Vandesande, G.A. Orban, C.W. Heizmann, and R. Pochet (1991b) Calcium binding proteins as molecular markers for cat geniculate neurons. Exp. Brain Res. *83:*513–520.

Freund, T.F. (1989) GABAergic septohippocampal neurons contain parvalbumin. Brain Res. *478:*375–381.

Freund, T.F., G. Buzsaki, A. Leon, K.G. Baimbridge, and P. Somogyi (1990) Relationship of neuronal vulnerability and calcium binding protein immunoreactivity in ischemia. Exp. Brain Res. *83:*55–66.

Gulyas, A.I., K. Toth, P. Danos, and T.F. Freund (1991) Subpopulations of GABAergic neurons containing parvalbumin, calbindin D28k, and cholecystokinin in the rat hippocampus. J. Comp. Neurol. *312:*371–378.

Hendrickson, A.E., J.F.M. Van Brederode, K.A. Mulligan, and M.R. Celio (1991) Development of calcium binding proteins parvalbumin and calbindin in monkey striate cortex. J. Comp. Neurol. *307:*626–646.

Hendry, S.H.C., E.G. Jones, P.C. Emson, D.E.M. Lawson, C.W. Heizmann, and P. Streit (1989) Two classes of cortical GABA neurons defined by differential calcium binding protein immunoreactivities. Exp. Brain Res. *76:*467–472.

Huntley, G.W., and E.G. Jones (1990) Cajal-Retzius neurons in developing monkey neocortex show immunoreactivity for calcium binding proteins. J. Neurocytol. *19:*200–212.

Johansen, F.F., N. Tonder, J. Zimmer, K.G. Baimbridge, and N.H. Diemer (1990) Short-term changes of parvalbumin and calbindin immunoreactivity in the rat hippocampus following cerebral ischemia. Neurosci. Lett. *120:*171–174.

Kamphuis, W., E. Huisman, W.J. Wadman, C.W. Heizmann, and F.H. Lopes da Silva (1989) Kindling induced changes in parvalbumin immunoreactivity in rat hippocampus and its relation to long-term decrease in GABA-immunoreactivity. Brain Res. *479:*23–34.

Katsumaru, H., T. Kosaka, C.W. Heizmann, and K. Hama (1988) Immunocytochemical study of GABAergic neurons containing the calcium-binding protein parvalbumin in the rat hippocampus. Exp. Brain Res. *72:*347–362.

Kobayashi, K., P.C. Emson, C.Q. Mountjoy, S.N. Thornton, D.E.M. Lawson, and D.M.A. Mann (1990) Cerebral cortical calbindin D28k and parvalbumin neurones in Down's syndrome. Neurosci. Lett. *113:*17–22.

Kosaka, T., H. Katsumaru, K. Hama, J.-Y. Wu, and K.W. Heizmann (1987) GABAergic neurons containing the Ca^{2+}-binding protein parvalbumin in the rat hippocampus and dentate gyrus. Brain Res. *419:*119–130.

Lewis, D.A., and J.S. Lund (1990) Heterogeneity of chandelier neurons in monkey neocortex: Corticotropin-releasing factor- and parvalbumin-immunoreactive populations. J. Comp. Neurol. *293:*599–615.

Lewis, D.A., M.J. Campbell, and J.H. Morrison (1986) An immunohistochemical characterization of somatostatin-28 and somatostatin-$28_{1\text{-}12}$ in monkey prefrontal cortex. J. Comp. Neurol. *248:*1–18.

McDonald, A.J. (1982) Neurons of the lateral and basolateral amygdaloid nuclei: A Golgi study in the rat. J. Comp. Neurol. *212:*293–312.

McDonald, A.J. (1984) Neuronal organization of the lateral and basolateral amygdaloid nuclei in the rat. J. Comp. Neurol. *222:*589–606.

McDonald, A.J. (1985) Immunohistochemical identification of γ-aminobutyric acid-containing neurons in the rat basolateral amygdala. Neurosci. Lett. *53:*203–207.

McDonald, A.J., and K.G. Baimbridge (1990) Calcium binding protein containing neurons of the basolateral amygdala also exhibit GABA and cytochrome oxidase immunoreactivity. Soc. Neurosci. Abstr. *16:*431.

Millhouse, O.E., and J. DeOlmos (1983) Neuronal organizations in lateral and basolateral amygdala. Neuroscience *10:*1269–1300.

Mudrick, L.A., and K.G. Baimbridge (1989) Long-term structural changes in the rat hippocampal formation following cerebral ischemia. Brain Res. *493:*179–184.

Nitecka, L., and Y. Ben-Ari (1987) Distribution of GABA-like immunoreactivity in the rat amygdaloid complex. J. Comp. Neurol. *266:*45–55.

Nitsch, R., and C. Leranth (1991) Neuropeptide Y (NPY)-immunoreactive neurons in the primate fascia dentata; occasional coexistence with calcium-binding proteins: A light and electron microscopic study. J. Comp. Neurol. *309:*430–444.

Nitsch, R., E. Soriano, and M. Frotscher (1990) The parvalbumin-containing nonpyramidal neurons in the rat hippocampus. Anat. Embryol. *181:*413–425.

Ottersen, O.P., B.O. Fischer, E. Rinvik, and J. Storm-Mathisen (1986) Putative amino acid transmitters in the amygdala. In R. Schwarcz and Y. Ben-Ari (eds): Excitatory Amino Acids in Epilepsy. New York: Plenum Press, pp. 53–66.

Pitkänen, A., and D.G. Amaral (1991) Distribution of reduced nicotinamide adenine dinucleotide phosphate diaphorase (NADPH-d) cells and fibers in the monkey amygdaloid complex. J. Comp. Neurol. *313:*326–348.

Price, J.L., F.T. Russchen, and D.G. Amaral (1987) The limbic region. II: The amygdaloid complex. In A. Björklund, T. Hökfelt, and L.W. Swanson (eds): Handbook of Chemical Neuroanatomy, Vol. 5: Integrated Systems of the CNS, Part I. Amsterdam: Elsevier, pp. 279–388.

Rosene, D.L., N.J. Roy, and B.J. Davis (1986) A cryoprotection method that facilitates cutting frozen sections of whole monkey brains for histological and histochemical processing without freezing artifact. J. Histochem. Cytochem. *34:*1301–1315.

Seress, L., A.I. Gulyas, and T.F. Freund (1991) Parvalbumin- and calbindin D_{28k}-immunoreactive neurons in the hippocampal formation of the macaque monkey. J. Comp. Neurol. *313:*162–177.

Sloviter, R.S. (1989) Calcium-binding protein (Calbindin-D_{28k}) and parvalbumin immunocytochemistry: Localization in the rat hippocampus with specific reference to the selective vulnerability of hippocampal neurons to seizure activity. J. Comp. Neurol. *280:*183–196.

Sloviter, R.S., A.S. Sollas, N.M. Barbaro, and K.D. Laxer (1991) Calcium-binding protein (calbindin-D28K) and parvalbumin immunocytochemistry in the normal and epileptic human hippocampus. J. Comp. Neurol. *308:*381–396.

Smith, Y., A. Parent, L. Kerkerian, and G. Pelletier (1985) Distribution of neuropeptide Y immunoreactivity in the basal forebrain and upper brainstem of the squirrel monkey (*Saimiri sciureus*). J. Comp. Neurol. *236:*71–89.

Somogyi, P., T.F. Freund, and A. Cowey (1982) The axo-axonic interneuron in the cerebral cortex of the rat, cat and monkey. Neuroscience 7:2577–2607.

Stichel, C.C., W. Singer, and C.W. Heizmann (1988) Light and electron microscopic immunocytochemical localization of parvalbumin in the dorsal lateral geniculate nucleus of the cat: Evidence for coexistence with GABA. J. Comp. Neurol. *268:*29–37.

Van Brederode, J.F.M., K.A. Mulligan, and A.E. Hendrickson (1990) Calcium-binding proteins as markers for subpopulations of GABAergic neurons in monkey striate cortex. J. Comp. Neurol. *298:*1–22.

Waldvogel, H.J., R.L.M. Faull, M.N. Williams, and M. Dragunow (1991) Differential sensitivity of calbindin and parvalbumin immunoreactive cells in the striatum to excitotoxins. Brain Res. *546:*329–335.

Weiss, J.H., J-Y. Koh, K.G. Baimbridge, and D.W. Choi (1990) Cortical neurons containing somatostatin- or parvalbumin-like immunoreactivity are atypically vulnerable to excitotoxic injury *in vitro*. Neurology *40:*1288–1292.